University of Thessaly
School of Engineering
Department of Mechanical Engineering

ALUMINUM BASED SACRIFICIAL ANODES: COMPOSITION AND ELECTROCHEMICAL PERFORMANCE

by

KONSTANTINOS-PANAGIOTIS LIONTOS

Submitted in partial fulfillment of the requirements for the degree of
Diploma in Mechanical Engineering at the University of Thessaly

Volos, Greece, July 2021

Approved by the Committee on Final Examination:

Advisor Dr. Anna D. Zervaki
Lab Teaching staff, Department of Mechanical Engineering
University of Thessaly

Member Dr. Gregory Haidemenopoulos
Professor, Department of Mechanical Engineering
University of Thessaly

Member Dr. Alexis Kermanidis
Assistant Professor, Department of Mechanical Engineering
University of Thessaly

Acknowledgements

I would like to sincerely thank my thesis supervisor, Anna D. Zervaki, for her guidance, support and insightful comments throughout the course of this thesis.

I am forever grateful for the support and love my family has given me throughout the journey of my life, I love you all.

Aluminum based sacrificial anodes: Composition and electrochemical performance

Konstantinos-Panagiotis Liontos
Department of Mechanical Engineering, University of Thessaly

Supervisor: Dr Anna D. Zervaki

Abstract

Utilization of Sacrificial anodes is the prominent method of providing adequate Cathodic Protection for ships and offshore installations, due to their simplicity, structural integrity and standalone nature. Aluminum, Zinc and Magnesium sacrificial anodes have been developed for commercial use and their application is case-specific. In offshore marine applications, Aluminum is almost exclusively used, owing to its low cost, low density, high current capacity and the desirable, for the protection of steel structures in seawater, operating voltage range. Although Aluminum anodes have desirable properties, Pure Aluminum has the major drawback of rapidly forming a protective layer of Al_3O_2 on its surface when exposed to NaCl solutions, leading to passivation and as a result inadequate protection of the cathode. Therefore, aluminum anodes are alloyed with small amounts of elements in order to disturb the formation of the passive oxide film and avoid passivation. The way the disturbance of the oxide film is achieved, called activation mechanism, varies depending on the composition and the alloying elements. Although commercially available Aluminum sacrificial anodes offer adequate protection, the quest of improving on specific performance aspects is ongoing with researchers experimenting with new materials or conduct studies, from a new perspective, on already proven formulas with the purpose of improving upon them. In this Thesis, the effect of individual and multiple element additions on the electrochemical performance of Aluminum sacrificial anodes is investigated.

Keywords: Cathodic Protection, Aluminum sacrificial anodes, Seawater.

Contents

List of Figures

List of Tables

Chapter 1

Introduction

1.1 Thesis scope

The goal of this thesis is to present in a systematic and comprehensive way the effect of individual and multiple element additions on the electrochemical performance and corrosion behavior of Aluminum sacrificial anodes in seawater solutions.

An extended literature review has been conducted in order to record the results, identify the goals and therefore the motivation of researchers both in the past and in the present. The findings presented in this thesis span many decades and are conducted from research groups located in different geographic regions with varying backgrounds. The diversity of the research groups and their individual approaches on the issue of Cathodic protection with the use of sacrificial anodes, lead to the creation a knowledge database that covers the issue in a holistic way.

1.2 Thesis structure

This thesis is divided in 5 chapters. The topics covered in the following chapters are as follows:

- In Chapter 2 the theory of Galvanic Corrosion and the corrosion control method of Cathodic Protection with the use of sacrificial anodes are presented. The parameters influencing the magnitude of galvanic corrosion are presented in detail and the target values for the operation of sacrificial anodes are discussed.

- Chapter 3 contains the equations for the design of a Cathodic Protection system. The factors that influence the current density requirements and therefore the necessary number of anodes are also presented.
- In chapter 4 the findings from the literature review on the effect of individual and multiple element additions on the electrochemical performance and corrosion behavior of aluminum sacrificial anodes is presented
- Chapter 5, as the final chapter, summarizes the findings and outlines the future research trends

Chapter 2

Galvanic corrosion and cathodic protection

2.1 Galvanic Corrosion

Galvanic corrosion is an electrochemical form of corrosion that occurs when a metal or alloy is electrically coupled to another metal or conducting nonmetal in the same electrolyte (either in contact with each other or connected via conductive wire).

The following conditions must all be satisfied for Galvanic corrosion to occur:

1. Two metals/alloys or conducting nonmetals that possess different surface potentials.
2. A common electrolyte where the anode and cathode reside.
3. A common electrical path where the anode and cathode are electrically connected (either in contact with each other or connected via conductive wire)

If any of these conditions in not met, galvanic corrosion will not occur.

During galvanic coupling:

- corrosion of the less corrosion-resistant (more active) metal increases and the surface becomes anodic (Anode)

- corrosion of the more corrosion-resistant (more noble) metal decreases and the surface becomes cathodic (Cathode)

Corrosion occurs due to the formation of electrochemical cells. The electrochemical cell is driven by the potential difference between the dissimilar metals of the anode and the cathode.

The potential difference creates a current, called galvanic current, the direction of which is determined by the corrosion potentials of the coupled metals. The magnitude of the galvanic current can be calculated using Kirchhoff's 2^{nd} law, specifically:

$$I_{galv} = (E_c - E_a)/(R_e + R_m) \tag{2.1}$$

Where:

- E_c: polarized potential of cathode
- E_a: polarized potential of anode
- R_e: electrolyte resistance
- R_m: connection resistance

The rate of corrosion is the result of two opposing reactions, an anodic reaction where the metal gets oxidized releasing electrons and a cathodic one where Hydrogen gets reduced removing electrons from the anodic metal. Specifically, the following reactions take place in a galvanic couple:

- Oxidation (anodic reaction) that occurs at the Anode: $M \rightarrow M^{n+} + ne^-$
- Reduction (cathodic reaction) that occurs at the cathode and results in Hydrogen evolution (gas): $2H^+ + 2e^- \rightarrow H_2(\uparrow)$

In a corrosion cell, (see figure 2.1 metal ions formed from metal oxidation (cations) migrate from the anode to the cathode through the electrolyte. The electrons given off by this oxidation reaction move from the anode to the cathode through the electrical connection. Current flows from the cathode to the anode through the electrical connection and from the anode to the cathode in the electrolyte.

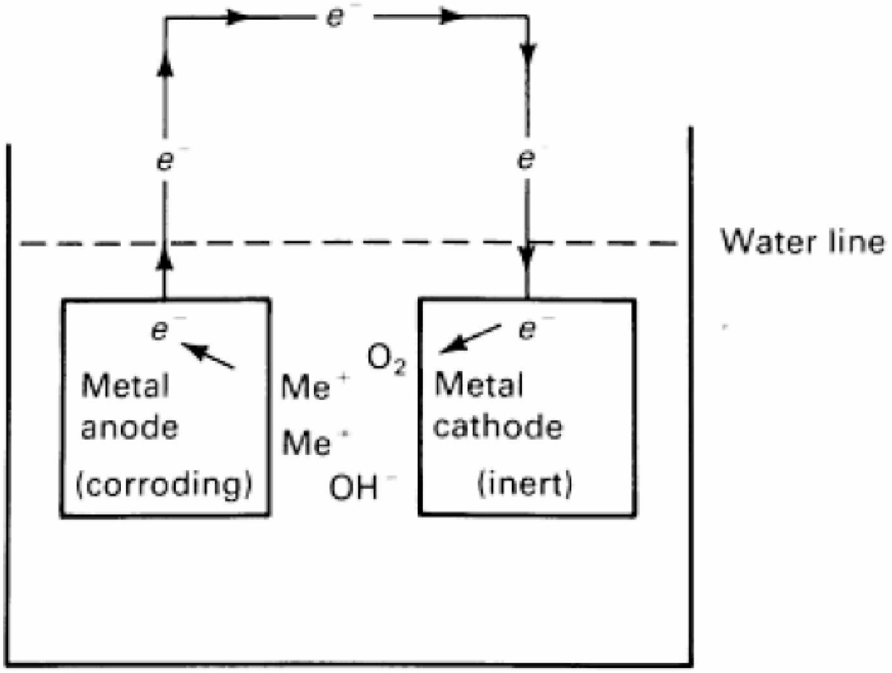

Figure 2.1: Representation of a Galvanic cell. ((Cramer and Covino, 2003))

The galvanic corrosion rate is affected by the following factors:

1. The potential difference between the metals or alloys

The rate of galvanic corrosion depends upon the difference in electrochemical potential of the two metals; the greater the difference, the faster the corrosion of the anodic metal will be. A quick way to predict the galvanic relationship of various metals is the Galvanic Series. Such a series is a list of freely corroding potentials of various metals and alloys in a common electrolyte, arranged in order of potential 2.2. The galvanic series is a useful tool for the prediction of the more active metal in a galvanic couple and also the separation between the two metals in the galvanic series offers a qualitative indication of the probable magnitude of the corrosive rate.

The limitations of the Galvanic series are:

- The rate of corrosion cannot be accurately determined for any given galvanic couple.

- Some metals/alloys exhibit both an active and passive state, with substantial difference in the potentials of both states (passivation). Some Galvanic Series tables do include data for both states.
- The data present in a Galvanic Series are valid strictly for the specific electrolyte that the measurements were conducted. Small variations in the composition of the electrolyte may cause extended variation on the performance of the metals/alloys present on the series.
- Potentials of most metals/alloys are not constant and during extended periods of use some variation in the anode's performance is to be expected. The galvanic Series does not incorporate time dependent information on the performance of the metals/alloys.

2. The nature of the environment - aqueous solutions

For the purposes of this master thesis only saline solutions, otherwise designated as either natural or artificial “Seawater”, have been investigated. “Natural Seawater” is a complex solution of inorganic, organic, and biological components. These components mean that solutions sampled directly from the ocean are not easily simulated or reproduced in the laboratory for corrosion-testing purposes. Furthermore, seawater directly sampled from the ocean is exhibiting corrosive behavior different from that of the water mass from which it was taken, because the various constituents, such as the living organisms and their dissolved organic nutrients, are in balance in the natural environment, a balance that changes soon after a seawater sample is isolated from the parent water mass. As a result, most researchers create “artificial seawater” solutions according to industry standards such as ASTM D1141 or simply NaCl solutions of varying concentrations. The major parameters that affect Galvanic Corrosion in natural seawater solutions are:

- Dissolved oxygen content: an increase in dissolved oxygen increases the corrosivity of seawater.
- Sea currents: greater relative speeds between the cathodic structure and the solution lead to a faster stripping of the protective films, coatings and inorganic growth (calcareous scale) exposing bare metal and increasing the rate of Galvanic corrosion.

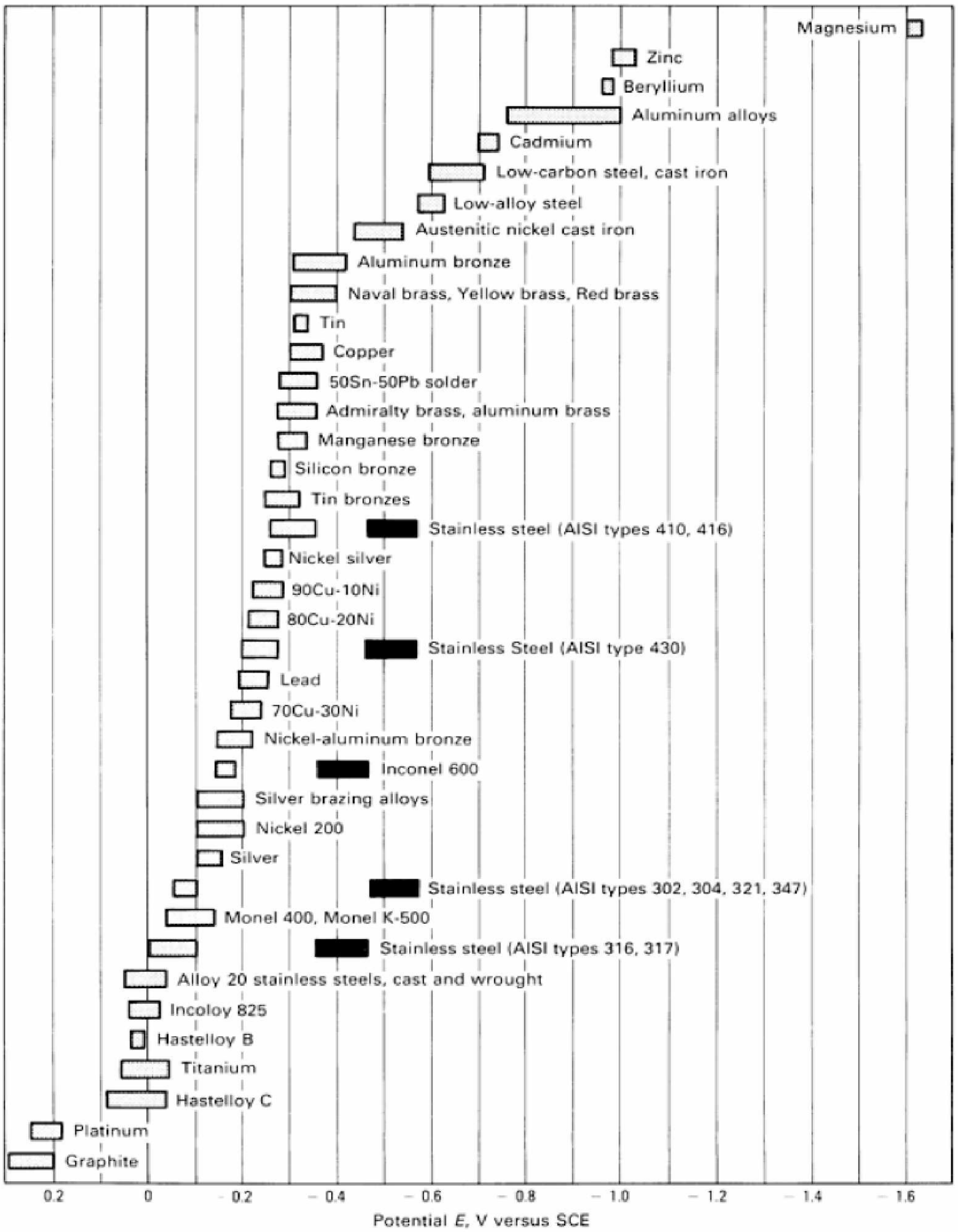

Figure 2.2: Galvanic Series.

- Temperature: an increase in temperature increases the corrosivity of seawater.
- Presence of coatings, marine growth, calcareous scale.
- Salinity: An increase in NaCl contents increases conductivity.
- PH and carbonate content: Both are considered factors which affect the formation of calcareous layers. The PH of seawater varies between 7.8-8.4 with lower PH values resulting to greater Galvanic corrosion rates.

3. The cathode/anode surface area ratio and distance within the electrolyte ((Swain, 1996))

Effect of area ratio:

- In a galvanic couple, given a constant current density requirement (A/m2) for the protection of the cathodic metal/alloy, an increase in the exposed cathodic surface area is translated in a linear current demand increase. The current demand must be satisfied by electrons released from the anode. Materials have a set current capacity ε (Ah/kg) and as a result, larger cathodic areas that result in increased current requirements, increase the rate of dissolution of the anode.
- If the cathode/anode surface ratio is highly unfavorable (cathode surface much greater that the anode surface), the anode will be rapidly consumed.
- If the cathode/anode surface ratio is highly favorable (anode surface is equal or greater that the cathode surface), the anode consumption rate is greatly reduced.

Effect of Distance:

- The physical distance of the galvanic couple in the common electrolyte is highly dependent on the electrolyte's conductivity.
- In highly conductive electrolytes, like seawater, the distance effect is negligible. Galvanically coupled materials or structures that are meters apart can still interact and the anode will provide sufficient current for the protection of the cathode.

2.2 Cathodic Protection with sacrificial anodes

Cathodic protection (CP) is a method used to protect metals/alloys that would readily corrode in their working environment. In essence, a galvanic couple is created by the introduction of a more active metal to serve as the anode and the structure to be protected as the cathode. Simply put, Cathodic Protection is a Galvanic corrosion process utilized in a controlled manner.

Cathodic protection is a corrosion control technique that is not intended to provide immunity to the cathode. The sheer number of sacrificial anodes and the current required to provide complete immunity to the cathode in any given scenario would be both economically and operationally unsustainable. The end goal of a well-designed Cathodic protection system is to reduce the rate of oxidation to the point that corrosion of the cathode becomes negligible without impairing the cathode's functionality.

The active metal introduced is called Sacrificial Anode, since it corrodes, "sacrifices", to protect the cathode. Sacrificial anodes are disposable and have a specific predetermined life expectancy. Periodically, sacrificial anodes must be inspected and replaced, depending on the specific case, from every few years to decades. ((Norske Veritas, 2010))

2.3 Performance values of sacrificial anodes

The performance of sacrificial anodes is dictated by their current capacity, anodic current efficiency and working potential.

Current capacity: The amount of current that 1kg of anode material can produce in one hour in steady state conditions. The measurement unit is "Ah/kg" and is symbolized as "ε".

Anodic current efficiency: The ratio of actual current capacity to theoretical current capacity. This value is a tool for the performance assessment of an anode against its maximum theoretical performance values. The absolute current capacity is the ultimate measure of an anode's performance.

Working potential: The potential of the anode in steady state conditions. Most sacrificial anodes require a "break-in" period, where both current capacity and potential values may vary significantly. After this period, both values remain relatively steady for extended periods of time. Towards the end of the anode's service time, potential will rise to more positive values, therefore preemptive replacement is mandatory, periodically, every few years depending on the application.

2.3.1 Target values for the CP of steel structures in seawater

- **300mV criterion**

Steel used in the shipping industry corrodes freely at potentials between -480mV to -650 mV against Saturated Calomel Electrode (SCE). Various empirical criteria are applicable for the required shift in potential needed in order to provide adequate Cathodic protection, the most prominent one being the 300mV potential Shift criterion. Specifically, the 300mV potential shift criterion, states that the sacrificial anode must shift the polarization potential of the formed galvanic couple by at least 300mV to the negative direction compared to the free corrosion potential of the cathode.

- **The problem of overprotection**

Excessively negative potentials, less than -800 mV but especially below -1000 mV (SCE), not only surpass the requirements for adequate cathodic protection, but the excessive currents may also cause issues due to excessive hydrogen evolution at the cathode. Specifically:

1. In cases where high strength steels are involved, the excessive hydrogen may diffuse in the metal's crystalline structure causing Stress corrosion cracking and/or embrittlement.
2. Dissolution (blistering and/or delamination) of cathode coatings due to the trapped hydrogen gas

In conclusion, the potential range necessary to protect steel in seawater typically lies between -730 mV to -950 mV (SCE), depending on the properties of the cathode. Potential values more negative than -1000 mV must be avoided due to overprotection concerns.

Important potential type definitions:

- Equilibrium or corrosion potential or open circuit potential (OCP): The potential measured when the test specimen is placed in a solution, without any external electrical connections is called open circuit potential. The measurement process of open circuit potentials is non-invasive since there is no current flow. The corrosion potential is defined as the potential that a sample has when no external current is applied. Corrosion potential, equilibrium potential and open circuit potential are identical. ((Gamry, 2021)) ((PalmSens, 2021))
- Operating potential or close circuit potential (CCP): The potential that the anode material exhibits when coupled with the cathode structure. In well-designed cathodic protection systems, the close circuit potential (CCP) and open circuit potential (OCP) values are almost equal due to the limited polarization of the anodic

material. Therefore, the open circuit potential values are generally provided and used in all calculations.

- Protection potential: The empirical potential that galvanic corrosion of a specific metal that is submerged in a specific electrolyte will practically cease.
- Driving voltage: The potential difference between the anode and the polarized cathodic structure. Practically, the driving voltage is the difference between the anode's open circuit potential and the required protection potential of the structure.

2.4 Overview of Mg, Zn and Al sacrificial anodes

On the galvanic series there are only three metals with more negative potential than steel: Magnesium, Zinc and Aluminum.

Added benefits of these three elements are:

- Commercial availability
- Non-toxic characteristics
- Stable performance and predictable behavior when properly alloyed
- Ease of production (casting)

Magnesium Anodes Pure Magnesium anodes have a very low working potential in the region of -1550 mV (SCE) and as a result are not suitable for the protection of offshore structures, due to overprotection concerns.

Pure magnesium forms a passive oxide film of $Mg(OH)_2$ in aqueous solutions without chlorides. In aqueous solutions with chlorides, the $Mg(OH)_2$ film is damaged and the anode quickly deteriorates due to pitting corrosion.

Magnesium anodes are primarily utilized in high resistivity terrains, like buried in soil or fresh waters. Additions of aluminum and zinc affect positively the potential and current capacities, while impurities such as iron, nickel, copper, and silicon have negative effects.

Performance wise, Mg has a low current efficiency of 55$\%$ and a theoretical current capacity of 1230 Ah/kg

Zinc Anodes Pure Zinc anodes have a working potential in the region of -1100 mV (SCE) and as a result are not suitable for the protection of offshore structures in seawater. Zinc anodes are primarily used in fresh waters and underground installations with resistivities higher than 2000 $ohm * cm$.

Performance wise, Zn has a high current efficiency of 95$\%$, and a theoretical current capacity of 820 Ah/kg

Aluminum Anodes Pure Aluminum anodes have a working potential of -1100 mV (SCE) but the spontaneous formation of a dense oxide film of Al_2O_3 in saline solutions reduces their potential to -780 mV (SCE), thus rendering pure aluminum not suitable for the protection of offshore structures in seawater.

Aluminum anodes are always alloyed in order to combat passivation and are used in low resistivity applications, like seawater.

Alloying pure aluminum with copper and nickel shift the potential in the positive direction, while zinc, magnesium, and cadmium decrease passivation and shift the potential the positive direction.

The presence of mercury, tin, and indium render aluminum anodes active throughout their service life, leading to uniform dissolution.

Performance wise, Aluminum sacrificial anodes have a high current efficiency of 90$\%$, and a theoretical current capacity of 2960 Ah/kg.

Figure 2.3 summarizes the potential values for Aluminum, Zinc and Magnesium based sacrificial anodes.

2.5 First application of Cathodic Protection on Ships

The first ever recorded application of sacrificial anodes took place in 1824 by Sir Humphry Davy. Davy was commissioned by the British navy to investigate and identify the reasons behind the corrosion of the copper sheeting attached to the wooden ship hulls and offer a viable solution. The ship that Davy experimented on was the HMS Samarang, an Atholl-class corvette launched in 1822. Copper sheeting was used in order to protect the ships from marine life, like barnacles and shipworm, that would attach

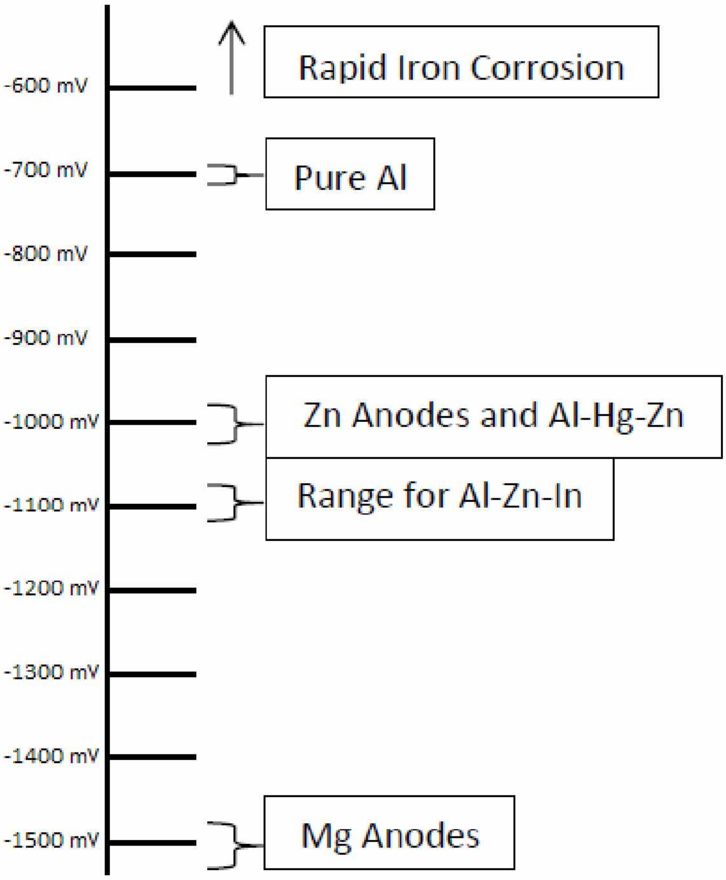

Figure 2.3: Typical potential values for Al, Zn and Mg based anodes ((7_b, 2016))

on the ship and cause issues ranging from excessive drag to physical deterioration of the wooden structure. Davy, based on his past experience and experimentation with the electrochemical properties of materials, proposed the attachment of pieces of tin, zinc and iron to the copper sheets. Sn, Zn and Fe are materials used with copper in voltaic batteries of the time. The proposed solution worked well, the oxidation of copper had seized, but a side effect was the growth of marine life on the copper sheets. The antifouling properties offered by the release of copper ions, had stopped as a result of the effective protection that zinc provided, leading to the wrong conclusion that the experiment had failed, banning the practice for many decades.

Chapter 3

External factors that affect anode performance and CP system service life

This chapter emphasizes on the factors that affect the cathodic current requirements throughout the service file of a Cathodic Protection system that utilizes Sacrificial Anodes.

The theoretically calculated service time is influenced by the protective coatings applied on the cathodic structures, the formation of calcareous scale and the ongoing reduction of the anode's mass. As a result, the calculation of a Cathodic Protection system's service life is a multivariant and time dependent function. The analytical formulae are presented in detail in reference documents ((Norske Veritas, 2010)), ((Committee, 1990)) and ((Cramer and Covino, 2003)) with case-specific coefficients for the theoretical calculations of CP systems. The analytical formulae are out of the context of this thesis.

3.1 Effect of coatings

Coatings or films are applied to the outer structure of a ship, both below and above water line, acting as physical barriers to corrosion. The marine industry's needs are constantly evolving and therefore new coating solutions are developed.

There are some prerequisites that must be satisfied by coating products, under development or in production, in order to be considered for offshore applications, specifically:

- The ability to serve their protective role for extended periods of time (at least the time in between drydocking periods).
- The ability of maintaining a high degree of adhesion to the underlying metallic surface, which is achieved via surface treatment.
- The coatings must be non-reactive or minimally reactive with seawater for environmental reasons (depending on the presence and toxicity of antifouling agents in the paint).
- Offer adequate antifouling protection.
- The ability to resist mechanical damage that could possibly expose the underlying metal.
- Offer a smooth and sleek finish to reduce drag.

Generally, Cathodic Protection systems using sacrificial anodes, that are not used in conjunction with coatings are not efficient solutions. The coatings applied to the metal structures reduce the diffusion rate of oxygen and as a result less current is needed to polarize the metal cathodically.

Types of coatings:

- Non-metallic coatings drastically reduce the Cathodic current demand required for the protection of a structure and hence, the required anode weight. For weight-sensitive structures with a long design life, the implementation of non-metallic coatings in a cathodic protection system is likely to give the most cost-effective corrosion control.
- Metallic coatings based on zinc or aluminium can be used in Cathodic protection systems but offer no advantage in decreasing the current demand requirements for the protection of the coated structures. Zinc-rich coatings are unsuitable for application with Cathodic protection systems due to their susceptibility to cathodic disbandment.

In order to quantify the protective action of coatings on bare metal structures, the coating breakdown factor (fc) is introduced: The coating breakdown factor (fc) describes the anticipated reduction in cathodic current density due to the application of an electrically insulating coating and is a function of coating properties, operational parameters and time. The coating breakdown factor is expressed as:

$$fc = a + b * t \tag{3.1}$$

where:

- t: the years since coating application.
- a and b: constants that are dependent on coating properties and the environment.

When $fc = 0$, the coating is 100% electrically insulating, thus decreasing the cathodic current density requirement to zero, while $fc = 1$ means that the coating has no current reducing properties. In practice, the expected value of fc lies between 0 and 1, partially reducing the current requirements.

3.2 Effects of the formation of calcareous scale and marine life

On offshore applications, organic and/or inorganic growths may develop. In ships there should be no such growths present. There are two categories of growths that are of interest, calcareous scale and marine life.

- Calcareous Scale

A consequence of Cathodic Protection applications in seawater is the formation of a calcareous layer, consisting of calcium carbonate ($CaCO_3$) and magnesium hydroxide ($Mg(OH)_2$), on bare metal surfaces 3.1. The thickness is typically of the order of 0.1 mm, but thicker deposits have been observed. This scale is beneficial since it is protective and nonconducting, reducing as a result the cathodic current density required for adequate cathodic protection.

The formation of calcareous scales requires a high initial current density in the early operational period. Once the calcareous scale is formed, the subsequent current requirements are reduced.

The build-up process of calcareous scales is a complex topic. High current densities may lead to excessive hydrogen evolution that can rupture the scale exposing bare metal, while very low current densities will not promote the formation of calcareous scales in the extent necessary for the reduction in current density to be met.

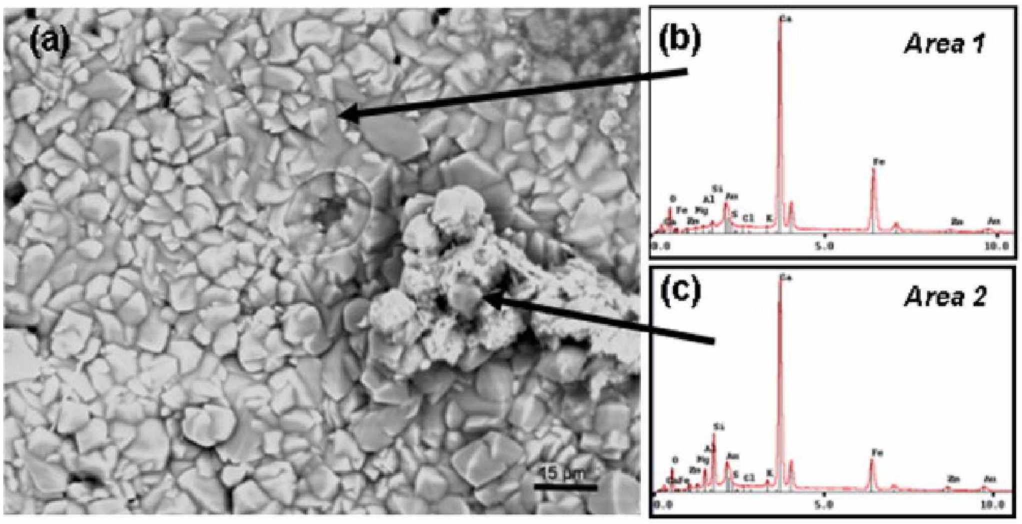

Figure 3.1: SEM image of Calcareous scale.

- Marine life

Plants and living organisms adhere to the protective coating of submerged structures, leading to fouling effect 3.2. Fouling effect reduces the diffusion of oxygen to the metal surface and at the same time forms an acidic environment due to the biological byproducts of the living organisms, leading to increased corrosion and increased drag as a result.

All paints used for the coating of ships and submerged structures have some form of antifouling action. In essence these coatings are created to slowly deteriorate releasing harmful ingredients rendering the submerged surfaces poisonous for marine life.

Figure 3.2: Marine life.

3.3 Current density requirements and total current demand

The term Current density refers to the cathodic protection current per unit surface area (A/m2) required for the adequate protection of a bare metal surface. There are 3 specific types of current densities that are of interest (also called design current densities), the initial, final and average. Specifically:

- Initial: This is the current density required to effect polarization on the exposed bare steel surface. Some rusting and/or millscale on the bare surface is assumed. The initial current density is the highest of the three, due to the absence of calcareous scales and marine growth. The goal of the initial current density is to form calcareous scales on the cathodic surface in a short time period.

- Final: This is the current density required for the protection of the metal surface after marine growth and calcareous scales are established. An appropriate final current density value will ensure that the potential will remain in the desired region throughout the design life of the system.

- Average (or maintenance): This is the current density required for the adequate protection of the system once it has reached its steady state potential. The average current density is used to calculate the minimum mass of anode material for the protection of the structure for a specified design life.

As sacrificial anodes get consumed, their surface area becomes smaller, increasing their anodic resistance. Therefore, sacrificial anodes reach a critical point where they can no longer offer adequate cathodic protection. This point is case specific for different geometries and is expressed with the utilization factor.

The utilization factor (u) is the $\%$ of the initial anode's mass that can provide adequate cathodic protection. When an anode is consumed to its utilization factor, the current capacity delivery becomes unpredictable and the anode itself structurally unstable, creating the need for replacement before the entirety of the anode is consumed. Typical values for the utilization factor (although highly dependent on the anode's geometry, proximity to the cathodic structure and insert placement) are in the 85% region.

3.3.1 Total current demand calculation

The first step in the design process of cathodic protection systems is the determination of the total current demand (Ic) that the sacrificial anodes must provide. ((Swain, 1996))

A cathodic structure may consist of surfaces with different properties and current density requirements. The current demand of a single surface is calculated by multiplying the individual surface area (Ac) by the relevant design current density (ic) and the coating breakdown factor (fc):

$$Ici = Ac * ic * fc \tag{3.2}$$

Where:

- Ici: current demand of individual surface (A)
- Ac: total surface area ($m2$)
- ic: is the relevant current density of the surface (A/m^2).
- fc: coating breakdown factor

For multiple surfaces with different properties, the total current density is: $Ic = Ic1 + Ic2 + Ic3\ldots$ An example of the anticipated current density requirements for the protection of ships is presented in Figure 3.3

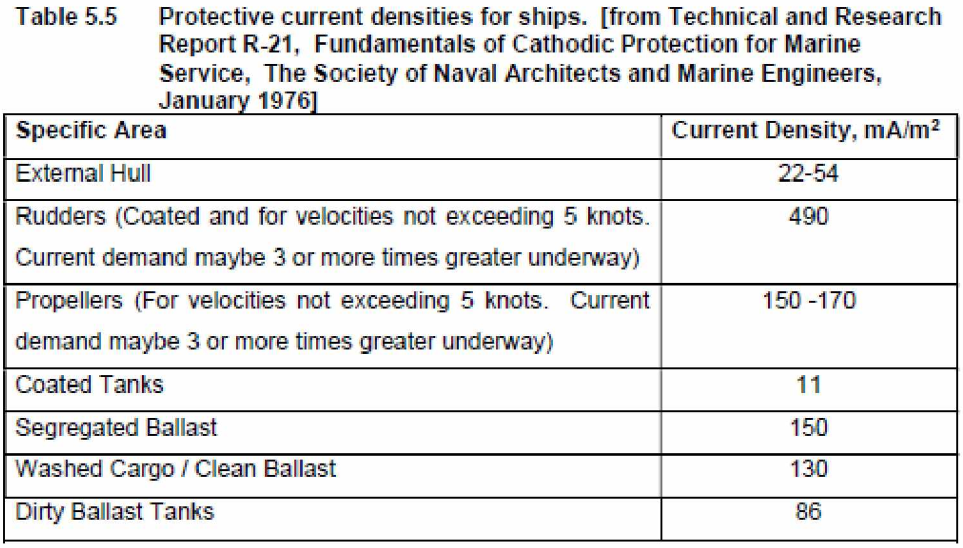

Table 5.5 **Protective current densities for ships. [from Technical and Research Report R-21, Fundamentals of Cathodic Protection for Marine Service, The Society of Naval Architects and Marine Engineers, January 1976]**

Specific Area	Current Density, mA/m²
External Hull	22-54
Rudders (Coated and for velocities not exceeding 5 knots. Current demand maybe 3 or more times greater underway)	490
Propellers (For velocities not exceeding 5 knots. Current demand maybe 3 or more times greater underway)	150 -170
Coated Tanks	11
Segregated Ballast	150
Washed Cargo / Clean Ballast	130
Dirty Ballast Tanks	86

Figure 3.3: Current density for various ship components ((Swain, 1996))

3.4 Design process of Cathodic protection systems and number of anodes calculation

Properly designed Cathodic Protection systems must provide the necessary current demand for the protection of a cathodic structure, throughout the designed service life of the system.

The design of Cathodic protection systems that use sacrificial anodes introduce a new set of restrictions and challenges. Specifically:

1. Calculation of the number of anodes needed to provide the required total current.
2. Calculation of the total anode mass required to meet the design life requirements.
3. The placement of the anodes on the cathodic structure, in order to provide uniform current distribution.

4. Minimize the adverse effects from the physical presence of the anodes, such as drag or increased weight.
5. Ensure the above criteria are met while using anode geometries and sizes that are commercially available.

The total number of anodes is calculated separately for the first and second criteria and the biggest resulting number of anodes will be used. The following examples assume a steady current density, coating breakdown factor and driving voltage.

3.4.1 Current demand criterion

The specific current output (Ia) of a single sacrificial anode is calculated as:

$$Ia = \Delta\mathrm{E}/R_{\alpha} \tag{3.3}$$

Where:

- $\Delta\mathrm{E}$: driving voltage (V)
- R_a: anode resistance (Ohm)

The total current needed for cathodic protection must be provided by the sacrificial anodes. Therefore, the total number of anodes (n) is determined by dividing the total current needed for cathodic protection (Ic) with the current output of each anode (Ia):

$$n = Ic/Ia \tag{3.4}$$

3.4.2 Design Life criterion

The total number of anodes must also be determined by the total mass required for the cathodic protection system to achieve a specific service life. The design life of a CP system is usually predetermined and application specific. Sacrificial anodes on ships are changed with every dry docking of the ship. ((Norske Veritas, 2010))

For a specific service life, the total anode mass is calculated as:

$$Ma = (Icm * tf * 8760)/(u * \varepsilon) \tag{3.5}$$

Where:

- Ma: anode mass (kg)
- Icm: current withdrawn (A)
- tf: expected years of service (years)
- 8760 is the total number of hours in one year
- u: utilization factor
- ε: current capacity (Ah/kg)

As a result, the number of anodes (n) is determined by dividing the total required anodic mass (Ma) with the mass of a single anode (m):

$$n = Ma/m \tag{3.6}$$

A properly designed Cathodic Protection system must satisfy both the current demand and service life criteria, therefore the total number of anodes will be equal to the highest calculated number of anodes from the two criteria.

Chapter 4

Composition and performance of Aluminum Sacrificial anodes

Aluminium anodes are attractive options for offshore applications, due to their high current capacity, low density, commercial availability, reasonable cost and stand-alone nature.

The first step in commercializing aluminum was the invention of the Hall–Héroult process in 1886, the major industrial process for aluminum production. The process is named after its inventors Charles Martin Hall and Paul Héroult, who simultaneously and independently invented it.

Despite its low density and resistance to corrosion, the aluminum produced was not suitable for structural applications up until the early 1900s when Alfred Wilm discovered the age-hardening process. In the 1930s aluminum was used extensively in structural applications but it would take another 30 years for the first application of aluminum as sacrificial anode material. The reason for this delay was pure aluminum's inability to readily corrode in saline solutions, due to the formation of a stable protective film, leading to passivation.

A milestone study in the performance of aluminum based sacrificial anodes was published by Reding and Newport in 1966. Reding and Newport experimented with aluminum-based alloys containing up to three different alloying elements from a pool of 37 elements, creating in total, 2500 unique compositions.

The researchers concluded that elements such as Mg, Zn, Cd, Ga, In, Hg and Sn were effective depassivators of aluminum in saline solutions. Elements such as Hg, Cd, Pb

Table 4.1: Aluminum purity specification ((Lindsay, 2014)).

Designation	Aluminum %
Commercial purity	99.5-99.79
High purity	99.8-99.949
Super purity	99.950-99.9959
Extreme purity	99.9960-99.9990
Ultra purity	>99.9990

even though proven to be beneficial, pose great threat to harbor and marine ecosystems due to their toxicity and therefore systematic efforts have been made for them to be replaced. The findings of their study are still relevant today and formed the knowledge foundation for the numerous studies that have been conducted since. Modern research is not targeted exclusively on the discovery of new high-performing compositions, researchers are interested in gaining insight on the activation mechanisms of the various depassivating elements. Commercially available, environmentally friendly, non-toxic and cast friendly elements are the main candidates for the high-performance sacrificial anodes that monopolize researcher's resources.

4.1 Alloying elements and impurities

The constituent elements of anode materials, other than the base metal, are either deliberate alloying additions or impurities.

- Alloying Elements

Alloying elements are deliberate additions to the base metal during the melting process. Each alloying element gives specific characteristics to the resulting alloy and the percentage of each element is precisely measured.

- Impurities

"Pure" aluminum alloys are classified into categories based on the percentage of impurity contents, as seen in Table 4.1:

High purity aluminum exhibits great corrosion behavior, due to the homogeneity of its structure. The presence of impurities leads to the formation of local electrochemical cells, cathodic areas within the alloy that create heterogeneity, leading to high self-corrosion rates and faster corrosion rates overall.

As an example, Iron impurity in Aluminum with a concentration of as little as 0.02% can cause a decrease in corrosion resistance of the base metal.

An important aspect in the production of sacrificial anodes is the cost of raw material. High purity aluminum is more expensive than commercial purity aluminum and as a result a compromise is made between desirable properties and cost. A viable option is to choose a commercial purity alloy and combat the adverse effects of impurities with specific alloying elements.

4.2 A brief overview of Testing methods and reference electrodes

The performance of aluminum-based sacrificial anode alloys is evaluated via electrochemical testing methods and against specific reference electrodes. The most important electrochemical tests are:

- Galvanostatic
- Potentiostatic
- Potentiodynamic and Cyclic Polarization
- Electrochemical Impedance Spectroscopy (EIS)

The methodology of these tests is based on protocols, like the ASTM testing methods. This way, the results obtained from different researchers, even many decades apart, are relevant and comparable.

In this chapter, information will be provided on the testing methods. The exact testing methodology is out of context for this master thesis.

4.2.1 Reference electrodes

During electrochemical tests, various potentials of the metal specimen under investigation are measured against reference electrodes. Since the potential of reference electrodes is known, it is possible, once a potential target value is specified for a metal specimen against a specific reference electrode, to calculate the exact potential against other reference electrodes.

The recommended protection potential values of steel in seawater for various reference electrodes are listed in Table 4.2:

Table 4.2: Protection potential of steel in seawater for various Reference Electrodes ((Bardal, 2004)).

Reference Electrode	Protection Potential (mV)
$Cu/CuSO_4$	–850
Ag/AgCl/seawater	–800
SCE	–780
SHE	–530
Zn	–250

The results obtained from Ag/AgCl/seawater and Saturated Calomel Electrode (SCE) are equivalent. In this thesis, all potential values are measured against SCE, unless otherwise noted.

4.2.2 Potentiostatic tests

Electrochemical tests are conducted on small metallic samples (few cm^2 surface area), submerged in a specific electrolyte. The sample and the solution are as close as possible, if not identical, to their real-world counterparts in an effort to produce an accurate simulation model. Electrodes, that are connected to a potentiostat, are inserted in the solution.

The potentiostat allows the user to accurately change the applied potential on the metal sample (input) and measure the changes in the current value (output) as a function of potential.

Potentiostatic tests are also referred as “controlled-potential” polarization. The process of applying a potential on the sample different than its open circuit potential, is called polarization. The data collected are used to model the corrosion behavior of the metal. ((Gamry, 2021))

4.2.3 Galvanostatic tests

During Galvanostatic testing, a constant current is applied to the sample (input) and potential values are recorded (output). The current value applied is calculated by multiplying the total area of the test sample by a specific current density (measured in A/m^2).

Galvanostatic tests are also referred as "controlled-current" polarization and are used in order to investigate of the corrosion of a sample under constant current conditions. ((Gamry, 2021))

4.2.4 Potentiodynamic tests

Potentiodynamic tests are used to study the corrosion behavior of surfaces. During potentiodynamic testing the potential applied to the test sample is swept across a predetermined potential range, with specific step. For every potential value the corresponding current value is recorded via a potentiostat and the final results are plotted in a "potential vs current" diagram. ((Gamry, 2021))

Remarks on the distinct regions of the potentiodynamic diagram (Figure 4.1)

- At around -550mV the current drops sharply to a local low. The corresponding potential value is the Open Circuit Potential (red box), where the total anodic current equals the total cathodic current.
- For potential values above the OCP, oxidation of the metal occurs and the maximum corrosion current density (Icp) is reached. The potential corresponding to the Icp is called passivation potential (Epass)
- Any Potential increase above the passivation potential, places the metal in the passive region and decreasing current densities are recorded until the passive current density (Ip) is reached.
- Any Potential increase (from the Ip corresponding potential), will lead to increased current densities attributed to oxygen development or pitting at the surface (transpassivity region)

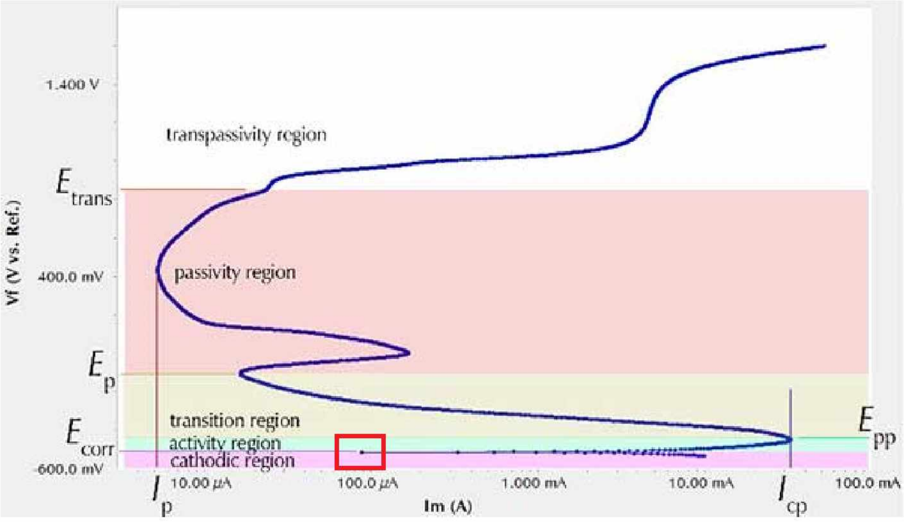

Figure 4.1: Example of a Potentiodynamic diagram ((Gamry, 2021)).

4.2.5 Cyclic polarization method

Both in Cyclic polarization tests and potentiodynamic tests the potential applied is swept across a predetermined potential range. The difference between the two test methods is that the potential is swept back to its original value in Cyclic polarization tests. ((Gamry, 2021))

Both testing methods are used to study the corrosion behavior of surfaces, although in the cyclic polarization method, since the sample surface is subjected to changes on the initial sweep, during the return to the original potential value the data do not superimpose, as seen on Figure 4.2.

4.2.6 Electrochemical Impedance Spectroscopy (EIS)

Electrochemical Impedance Spectroscopy is a complex and highly sensitive electrochemical testing method that can identify miniscule differences in the state of the tested samples and therefore provide unique insight to researchers. Specifically, EIS makes the identification of the influence of different mechanisms possible (i.e. electron transfer resistance or double layer capacity) and its high surface sensitivity allows researchers to

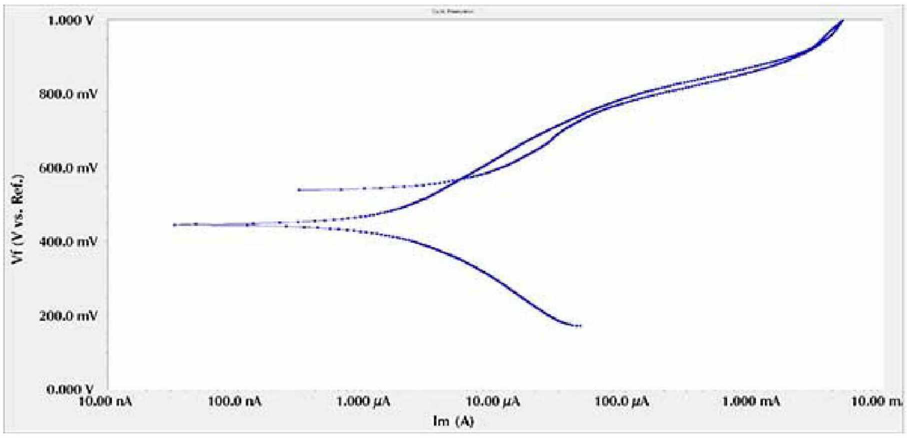

Figure 4.2: Example of Cyclic polarization diagram ((Gamry, 2021)).

observe small changes in the surface of samples that would be otherwise impossible to study, such as the effectiveness of coatings. ((PalmSens, 2021))

The testing method comprises of the application of a small sinusoidal potential or current of fixed frequency on the test sample, where the response is recorded and the impedance is calculated. The same process is repeated for different frequencies and the results are plotted on a Nyquist plot. Specific patterns on the Nyquist diagram (Figure 4.3) correspond to specific corrosion phenomena.

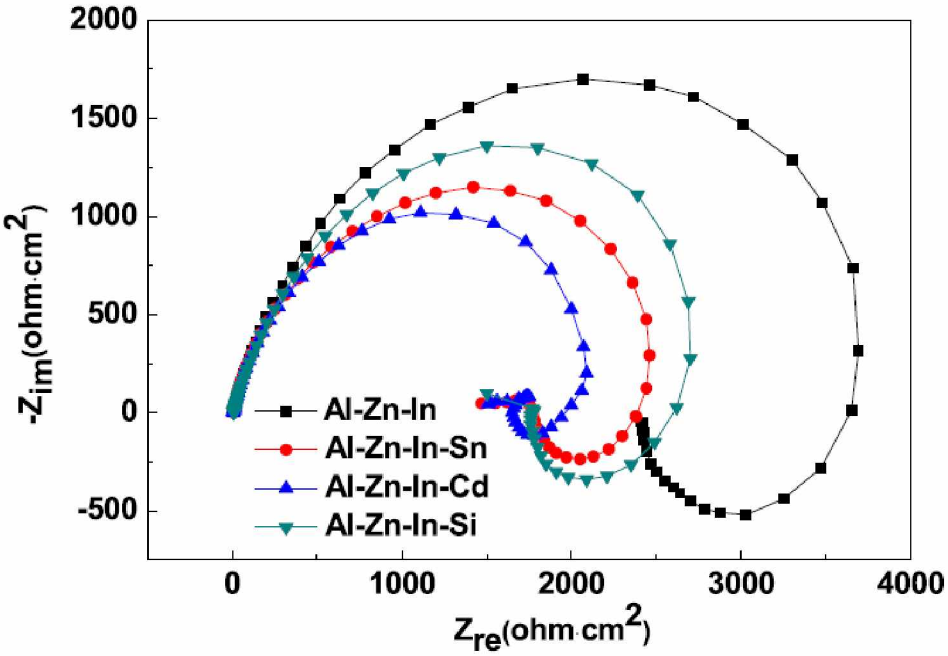

Figure 4.3: EIS data visualization in Niquist diagram. ((Xia et al.))

4.3 Alloying elements and Sacrificial anode compositions

The compositions of commercially available Aluminum sacrificial anodes in the past were Al-Zn-In, Al-Zn-Sn and Al-Zn-Hg. Indium, Tin and Mercury are effective depassivators of Aluminum in small concentrations and the resulting alloys have different properties. Specifically:

- Mercury activated Aluminum anodes exhibit high current capacities with the adverse effect of marine ecosystem pollution.
- Tin activated anodes exhibited inconsistent behavior and required additional heat treatment after casting to function properly.
- Indium activated anodes exhibit high electrochemical performance, uniform corrosion, ease of manufacture and non-polluting properties.

Al-Zn-In alloys are the predominant commercially available anodes for offshore applications, owing to their favorable characteristics. Extensive research has been conducted on the identification of the optimal composition and optimal casting parameters of Al-Zn-In alloys and their activation mechanisms in Saline solutions.

4.3.1 Effect of individual element additions on the performance of Aluminum sacrificial anodes

- Effect of Zinc addition: All Aluminum based sacrificial anodes are practically based on the binary Al-Zn system. In Al–Zn alloys, Zinc particles are rejected to interdendritic zones or grain boundaries. When the alloy gets polarized, preferential dissolution (galvanic corrosion and/or pitting corrosion) will initiate from the regions with high Zinc accumulation ((.A, 2018)). Even though high current density values are recorder from Al-Zn anodes, the high rate of corrosion results in a mediocre current efficiency ((Monzel and Druschitz, 2014)). Researchers concluded that Zinc addition is beneficial in compositions ranging between 0.5wt% and 10wt%, resulting in lower potentials and small improvements in current efficiency. Zinc content lower than 0.5wt% has no impact on performance, while concentrations greater than 10wt% have no additional benefits.

- Effect of Indium addition: Dissolved Indium is reduced in localized sites within the alloy. Indium must be in true electric contact with the base metal for activation to occur efficiently. At the localized Indium containing sites, chloride ion adsorption takes place and activation of the anode initiates. The activation mechanism of Indium containing Aluminum alloys is one of dissolution and redeposition ((Idusuyi and Oluwole, 2012)), ((Saremi et al., 2004)). Specifically, this mechanism suggests that Indium present in the aluminum anode dissolves and redeposits on the corrosion surface, leading to a local increase of Indium concentration and a periodic detachment of Indium rich zones from the oxide film, revealing the underlying active anode surface. The maximum solid solubility limit of Indium in Aluminum is low, at 0.02wt% ((Norris et al., 2000)). Indium additions as low as 0.004 wt% have a profound effect on the performance of the anode, leading to high current capacities and a shift of the potential to more negative values ((Monzel and Druschitz, 2014)). In Al-Zn-In alloys, corrosion initiation is located at grain boundaries where zones rich in In-Zn are identified. The contribution of Zinc in the activation of Al-Zn-In alloys can be attributed to the creation of an unstable oxide layer due to the presence of $ZnAl_2O_4$ areas on the oxide surface. The oxide layer facilitates the diffusion of Indium ions, preferential dissolution of Zinc and Indium accumulation at the surface. ((Saremi et al., 2004))

- Effect of Gallium addition: Breslin and Carroll ((Breslin and Carroll, 1992)) studied the effects of Gallium both as an alloying element and in the form of ions in solution. They concluded that activation of pure aluminium just from gallium ions in the solution is difficult and not feasible in the normal operating environment of the anodes. The slow deposition rate of gallium on the aluminum's surface means that critical activation levels will occur after many days of submergence in the ion-containing solution. Gallium, for activation of the anode to be achieved, must be present in solid solution to ensure a gallium-enriched surface at all times. The presence of gallium in the anode's surface assists chloride adsorption and once a sufficient degree of adsorption occurs, dissolution of the anode begins. Despite the fact that gallium ions cannot activate pure aluminum, an ion containing solution can aid the initial activation of Al-Ga alloys. Gallium content between 0.005wt% and 0.3wt% are beneficial for the activation of the anode and also raise its current efficiency. Gallium content lower than 0.005% has no impact on the performance of the anode, while gallium contents higher than 0.3wt% result in lower current efficiencies ((Toda et al., 1971)). Gallium is performing great as a low content addition in enhancing the performance of multiple element anodes, but anodes containing gallium as a sole element addition are underperforming.

- Effect of Tin addition: Al-Zn-Sn anodes were commercially available in the past but have been subsided by the more stable performance-wise Al-Zn-In anodes. An added issue with Al-Zn-Sn anodes that increases the production time and cost is the requirement for heat treatment after casting ((Crundwell, 2010)). The distribution of Tin in the anode, whether on grain boundaries or interdentritic regions, and as a result the performance characteristics of the resulting anode, is determined by casting parameters ((Saremi et al., 2004)). Researchers suggest that Tin creates additional cation vacancies by entering the Aluminum crystal matrix as Sn+4 ions ((Idusuyi and Oluwole, 2012)). Tin content between 0.05wt% and 1wt% is beneficial. Concentrations lower than 0.05wt% increase the anode potential and lower the anode current efficiency, while concentrations greater than 1wt% reduce the current efficiency of the anode ((Toda et al., 1971)).

- Effect of Bismuth addition: Bismuth addition to a baseline Al-Zn alloy enhances the current efficiency of the base alloy. Bismuth addition in Tin containing alloys renders the, otherwise necessary, heat treatment non-essential. Another positive side effect for Tin containing alloys is that Bismuth expands the aluminum matrix, increasing the solubility of Tin in Aluminum ((Idusuyi and Oluwole, 2012)). Experiments have shown that the proper Tin to Bismuth quantity ratio is one-to-one. Bismuth concentrations greater than 1wt% have the adverse effect of increasing the adhesion of corrosion products to the surface of the anode, making the removal of the outer oxide film difficult and as a result a reduction of the electrochemical performance of the anode is stated ((Toda et al., 1971)).

- Effect of Manganese addition: Manganese is a useful addition in Aluminum alloys containing Iron impurity because it counteracts its destructive effects (local cell creation) by creating Fe-Mn intermetallic compounds that are not cathodic. Manganese has limitations in its ability to counteract the detrimental effects of Iron, specifically up to a 0.22wt% Iron concentrations. The proper Manganese to Iron ratio is one to one and any excess of Manganese reduces the current capacity and increases the potential of the alloy ((Saeri and Keyvani, 2011)).

- Effect of Magnesium addition: Addition of Magnesium in Indium containing alloys aids the proper distribution of Indium within the Aluminum alloy and also refines the grain size, improving the current capacity of the alloy. The adhesion of the oxide film to the underlying surface is reduced and as a result the oxide film readily dissolves. ((Saeri and Keyvani, 2011))

4.3.2 Effect of multiple element additions on the performance of Aluminum sacrificial anodes

Gokulram ((.A, 2018)) prepared and experimented with an Al–5%Zn–5%Mg–0.1%Li alloy to study the effects of zinc addition on aluminum-based sacrificial anodes.

The alloy exhibited a mediocre current efficiency, a result attributed to the negative effects of secondary cathodic reactions within the anode (due to the high impurity concentrations of Fe and Cu) and also the formation of corrosion products on the corroding surface of the anode.

Table 4.3: Electrochemical performance of experimental compositions - Gokulram ((.A, 2018)).

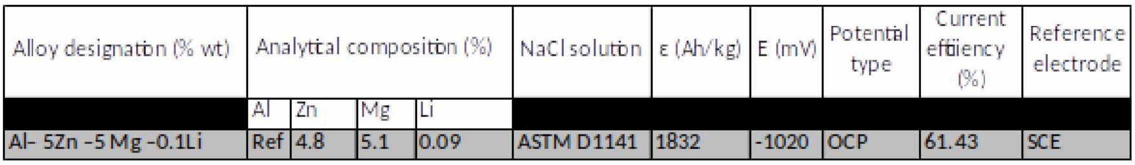

Alloy designation (% wt)	Analytical composition (%)				NaCl solution	ε (Ah/kg)	E (mV)	Potential type	Current efficiency (%)	Reference electrode
	Al	Zn	Mg	Li						
Al- 5Zn -5 Mg -0.1Li	Ref	4.8	5.1	0.09	ASTM D1141	1832	-1020	OCP	61.43	SCE

Norris et al ((Norris et al., 2000)) studied the electrochemical performance of commercially available Al-Zn-In anodes for the duration of one year. The operating potential of the anode remained relatively stable at approximately -1115 mV throughout the year, but the current efficiency steadily dropped from the initial value of 2420 Ah/kg to 2090 Ah/kg at the end of the year. The concentration of Fe and In on the corroding surface changes with time, a phenomenon directly attributed to the dissolution and redeposition activation mechanism.

Table 4.4: Electrochemical performance of experimental compositions – Norris et al ((Norris et al., 2000)).

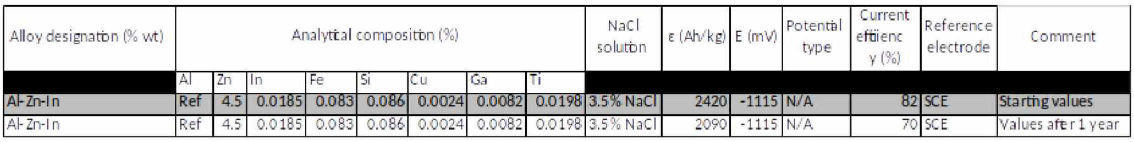

Alloy designation (% wt)	Analytical composition (%)								NaCl solution	ε (Ah/kg)	E (mV)	Potential type	Current efficiency (%)	Reference electrode	Comment
	Al	Zn	In	Fe	Si	Cu	Ga	Ti							
Al-Zn-In	Ref	4.5	0.0185	0.083	0.086	0.0024	0.0082	0.0198	3.5% NaCl	2420	-1115	N/A	82	SCE	Starting values
Al-Zn-In	Ref	4.5	0.0185	0.083	0.086	0.0024	0.0082	0.0198	3.5% NaCl	2090	-1115	N/A	70	SCE	Values after 1 year

Flamini and Saidman ((Flamini and Saidman, 2012)) investigated the influence of Ga addition in Al-Zn and Al-In alloys. Ga concentrations greater than 2.5wt% in Al-Zn-Ga alloys lead to excessively negative potentials, while Ga concentrations greater than 0.5wt% in Al-In-Ga alloys have the same effect. The activation of these alloys is attributed to an amalgam mechanism. This mechanism requires Ga to be uniformly distributed within the alloy.

Table 4.5: Electrochemical performance of experimental compositions – Flamini et al ((Flamini and Saidman, 2012)).

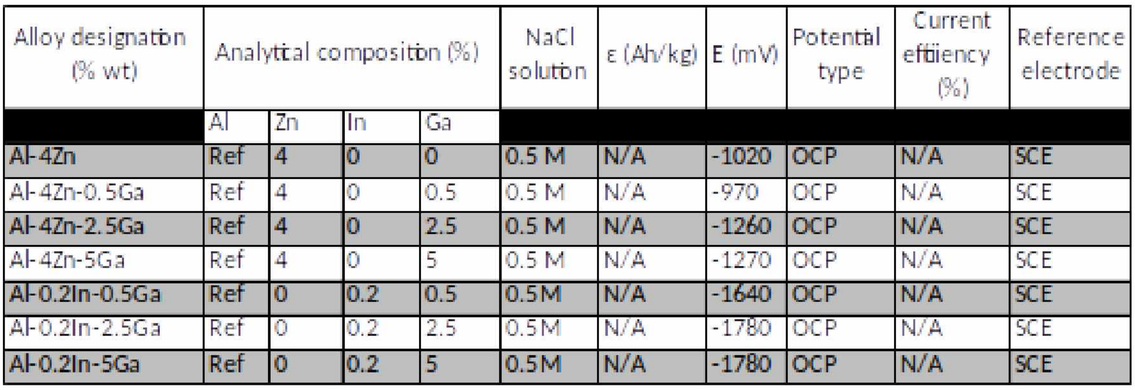

Alloy designation (% wt)	Analytical composition (%)				NaCl solution	ε (Ah/kg)	E (mV)	Potential type	Current efficiency (%)	Reference electrode
	Al	Zn	In	Ga						
Al-4Zn	Ref	4	0	0	0.5 M	N/A	-1020	OCP	N/A	SCE
Al-4Zn-0.5Ga	Ref	4	0	0.5	0.5 M	N/A	-970	OCP	N/A	SCE
Al-4Zn-2.5Ga	Ref	4	0	2.5	0.5 M	N/A	-1260	OCP	N/A	SCE
Al-4Zn-5Ga	Ref	4	0	5	0.5 M	N/A	-1270	OCP	N/A	SCE
Al-0.2In-0.5Ga	Ref	0	0.2	0.5	0.5M	N/A	-1640	OCP	N/A	SCE
Al-0.2In-2.5Ga	Ref	0	0.2	2.5	0.5M	N/A	-1780	OCP	N/A	SCE
Al-0.2In-5Ga	Ref	0	0.2	5	0.5M	N/A	-1780	OCP	N/A	SCE

Baker ((7_b, 2016)) created Al-0.1Ga alloys to study and characterize the corrosion behavior of the alloy. Tests were carried on the master heat and two subsequent remelts. Even though all alloys exhibited desirable potential values and high efficiencies, their inconsistent behavior is highly undesirable for commercial applications. The remelted alloys had increased nobility of grain boundaries and less inconsistency in their performance.

Table 4.6: Electrochemical performance of experimental compositions – Baker ((7_b, 2016)).

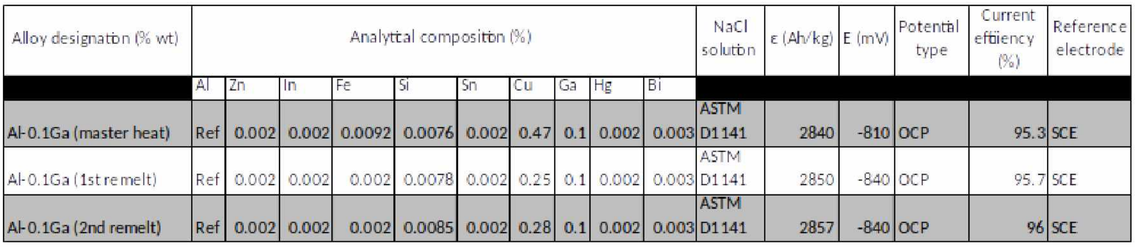

Alloy designation (% wt)	Analytical composition (%)										NaCl solution	ε (Ah/kg)	E (mV)	Potential type	Current efficiency (%)	Reference electrode
	Al	Zn	In	Fe	Si	Sn	Cu	Ga	Hg	Bi						
Al-0.1Ga (master heat)	Ref	0.002	0.002	0.0092	0.0076	0.002	0.47	0.1	0.002	0.003	ASTM D1141	2840	-810	OCP	95.3	SCE
Al-0.1Ga (1st remelt)	Ref	0.002	0.002	0.002	0.0078	0.002	0.25	0.1	0.002	0.003	ASTM D1141	2850	-840	OCP	95.7	SCE
Al-0.1Ga (2nd remelt)	Ref	0.002	0.002	0.002	0.0085	0.002	0.28	0.1	0.002	0.003	ASTM D1141	2857	-840	OCP	96	SCE

Monzel ((Monzel and Druschitz, 2014)) studied the electrochemical performance of Aluminum alloys containing Bi, Ga, In and Zn. The effect of each element in the corrosion behavior of their respective alloy in descending order is: In, Ga, Zn, Bi.

Table 4.7: Electrochemical performance of experimental compositions – Monzel ((Monzel and Druschitz, 2014)) .

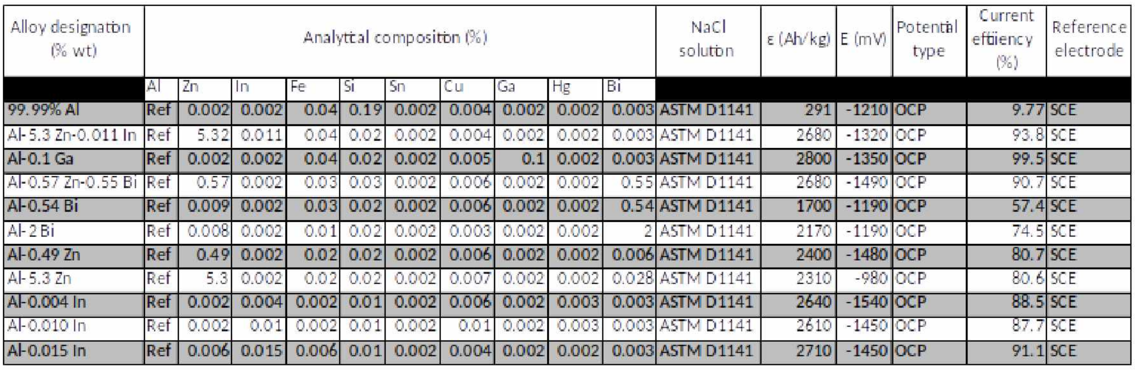

Alloy designation (% wt)	Analytical composition (%)										NaCl solution	ε (Ah/kg)	E (mV)	Potential type	Current efficiency (%)	Reference electrode
	Al	Zn	In	Fe	Si	Sn	Cu	Ga	Hg	Bi						
99.99% Al	Ref	0.002	0.002	0.04	0.19	0.002	0.004	0.002	0.002	0.003	ASTM D1141	291	-1210	OCP	9.77	SCE
Al-5.3 Zn-0.011 In	Ref	5.32	0.011	0.04	0.02	0.002	0.004	0.002	0.002	0.003	ASTM D1141	2680	-1320	OCP	93.8	SCE
Al-0.1 Ga	Ref	0.002	0.002	0.04	0.02	0.002	0.005	0.1	0.002	0.003	ASTM D1141	2800	-1350	OCP	99.5	SCE
Al-0.57 Zn-0.55 Bi	Ref	0.57	0.002	0.03	0.03	0.002	0.006	0.002	0.002	0.55	ASTM D1141	2680	-1490	OCP	90.7	SCE
Al-0.54 Bi	Ref	0.009	0.002	0.03	0.02	0.002	0.006	0.002	0.002	0.54	ASTM D1141	1700	-1190	OCP	57.4	SCE
Al-2 Bi	Ref	0.008	0.002	0.01	0.02	0.002	0.003	0.002	0.002	2	ASTM D1141	2170	-1190	OCP	74.5	SCE
Al-0.49 Zn	Ref	0.49	0.002	0.02	0.02	0.002	0.006	0.002	0.002	0.006	ASTM D1141	2400	-1480	OCP	80.7	SCE
Al-5.3 Zn	Ref	5.3	0.002	0.02	0.02	0.002	0.007	0.002	0.002	0.028	ASTM D1141	2310	-980	OCP	80.6	SCE
Al-0.004 In	Ref	0.002	0.004	0.002	0.01	0.002	0.006	0.002	0.003	0.003	ASTM D1141	2640	-1540	OCP	88.5	SCE
Al-0.010 In	Ref	0.002	0.01	0.002	0.01	0.002	0.01	0.002	0.003	0.003	ASTM D1141	2610	-1450	OCP	87.7	SCE
Al-0.015 In	Ref	0.006	0.015	0.006	0.01	0.002	0.004	0.002	0.002	0.003	ASTM D1141	2710	-1450	OCP	91.1	SCE

Jun-guang et al ((guang HE et al., 2011)) investigated the influence of Ga and Bi additions on the performance of a baseline Al-Zn-Sn alloy. The addition of Ga, Bi or both in the baseline Al-Zn-Sn alloy alters the microstructure from dendritic crystals to small equiaxed crystals. Individual additions of Ga and In create alloys with non-desirable corrosion characteristics, while the addition of both elements leads to uniform corrosion and high current efficiency.

Table 4.8: Electrochemical performance of experimental compositions – Jun-guang et al ((guang HE et al., 2011)) .

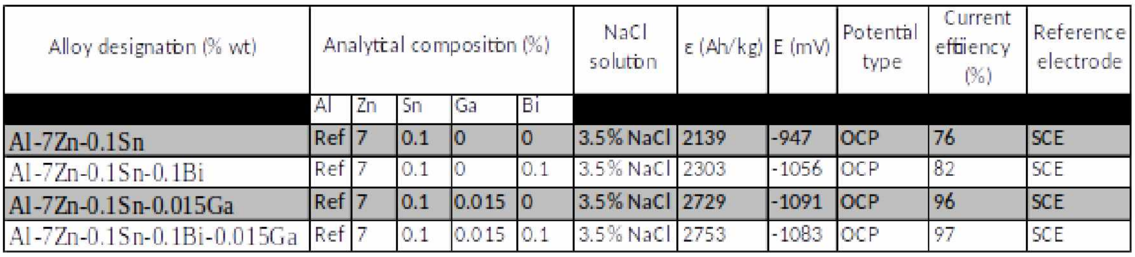

Alloy designation (% wt)	Analytical composition (%)					NaCl solution	ε (Ah/kg)	E (mV)	Potential type	Current efficiency (%)	Reference electrode
	Al	Zn	Sn	Ga	Bi						
Al-7Zn-0.1Sn	Ref	7	0.1	0	0	3.5% NaCl	2139	-947	OCP	76	SCE
Al-7Zn-0.1Sn-0.1Bi	Ref	7	0.1	0	0.1	3.5% NaCl	2303	-1056	OCP	82	SCE
Al-7Zn-0.1Sn-0.015Ga	Ref	7	0.1	0.015	0	3.5% NaCl	2729	-1091	OCP	96	SCE
Al-7Zn-0.1Sn-0.1Bi-0.015Ga	Ref	7	0.1	0.015	0.1	3.5% NaCl	2753	-1083	OCP	97	SCE

Toda et al ((Toda et al., 1971)) investigated the performance (potential and current efficiency) of Aluminum sacrificial anodes containing the elements Zinc, Tin, Bismuth and Gallium in varying amounts. The researchers concluded that Zinc addition is beneficial in concentrations between 0.5wt% and 10wt%. Zinc content lower than 0.5wt% had no impact on the performance, while Zinc content greater than 10wt% does not offer improvements.

Mance et al ((Mance A. and A., 1984)) investigated the performance characteristics of Al sacrificial anodes with additions of In and Tl. The alloys were created using high purity aluminum (5N) and technical purity aluminum (T).

Table 4.9: Electrochemical performance of experimental compositions – Toda et al ((Toda et al., 1971)).

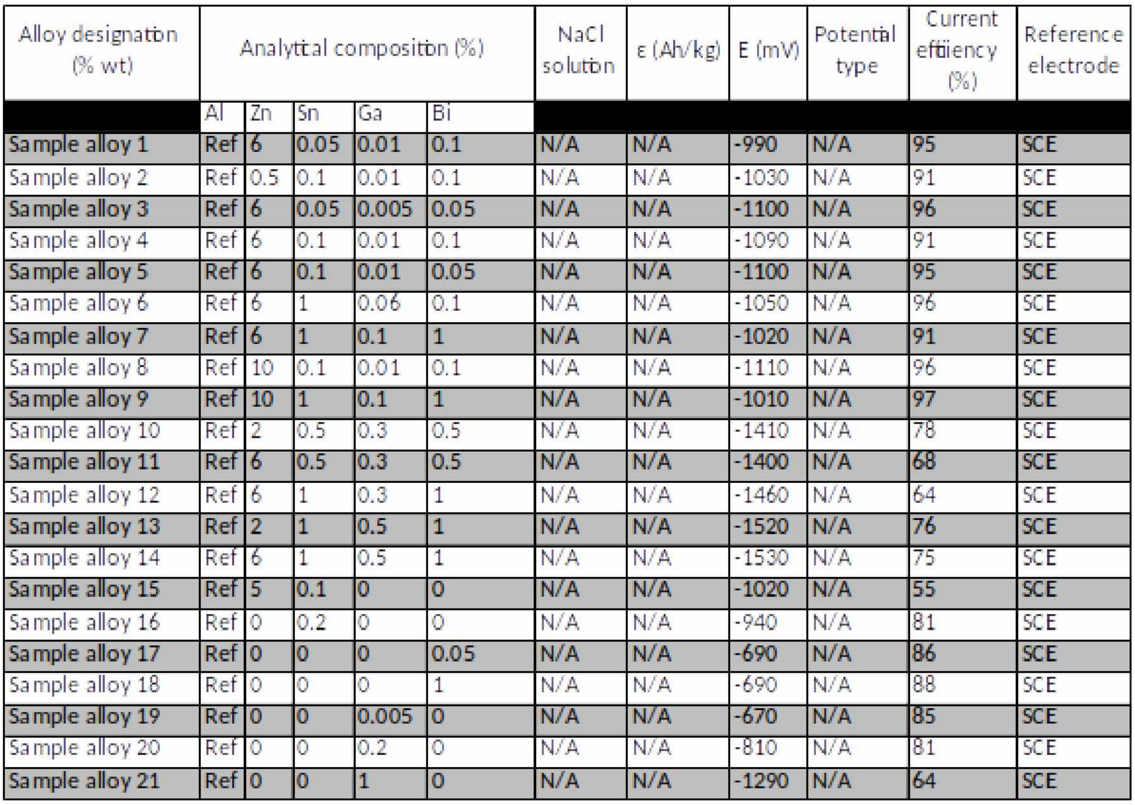

Alloy designation (% wt)	Analytical composition (%)					NaCl solution	ε (Ah/kg)	E (mV)	Potential type	Current efficiency (%)	Reference electrode
	Al	Zn	Sn	Ga	Bi						
Sample alloy 1	Ref	6	0.05	0.01	0.1	N/A	N/A	-990	N/A	95	SCE
Sample alloy 2	Ref	0.5	0.1	0.01	0.1	N/A	N/A	-1030	N/A	91	SCE
Sample alloy 3	Ref	6	0.05	0.005	0.05	N/A	N/A	-1100	N/A	96	SCE
Sample alloy 4	Ref	6	0.1	0.01	0.1	N/A	N/A	-1090	N/A	91	SCE
Sample alloy 5	Ref	6	0.1	0.01	0.05	N/A	N/A	-1100	N/A	95	SCE
Sample alloy 6	Ref	6	1	0.06	0.1	N/A	N/A	-1050	N/A	96	SCE
Sample alloy 7	Ref	6	1	0.1	1	N/A	N/A	-1020	N/A	91	SCE
Sample alloy 8	Ref	10	0.1	0.01	0.1	N/A	N/A	-1110	N/A	96	SCE
Sample alloy 9	Ref	10	1	0.1	1	N/A	N/A	-1010	N/A	97	SCE
Sample alloy 10	Ref	2	0.5	0.3	0.5	N/A	N/A	-1410	N/A	78	SCE
Sample alloy 11	Ref	6	0.5	0.3	0.5	N/A	N/A	-1400	N/A	68	SCE
Sample alloy 12	Ref	6	1	0.3	1	N/A	N/A	-1460	N/A	64	SCE
Sample alloy 13	Ref	2	1	0.5	1	N/A	N/A	-1520	N/A	76	SCE
Sample alloy 14	Ref	6	1	0.5	1	N/A	N/A	-1530	N/A	75	SCE
Sample alloy 15	Ref	5	0.1	0	0	N/A	N/A	-1020	N/A	55	SCE
Sample alloy 16	Ref	0	0.2	0	0	N/A	N/A	-940	N/A	81	SCE
Sample alloy 17	Ref	0	0	0	0.05	N/A	N/A	-690	N/A	86	SCE
Sample alloy 18	Ref	0	0	0	1	N/A	N/A	-690	N/A	88	SCE
Sample alloy 19	Ref	0	0	0.005	0	N/A	N/A	-670	N/A	85	SCE
Sample alloy 20	Ref	0	0	0.2	0	N/A	N/A	-810	N/A	81	SCE
Sample alloy 21	Ref	0	0	1	0	N/A	N/A	-1290	N/A	64	SCE

Thallium had no major effects on the properties of the alloys, while the effects of In and Tl additions were less noticeable in technical purity aluminum.

Table 4.10: Electrochemical performance of experimental compositions – ((Mance A. and A., 1984)).

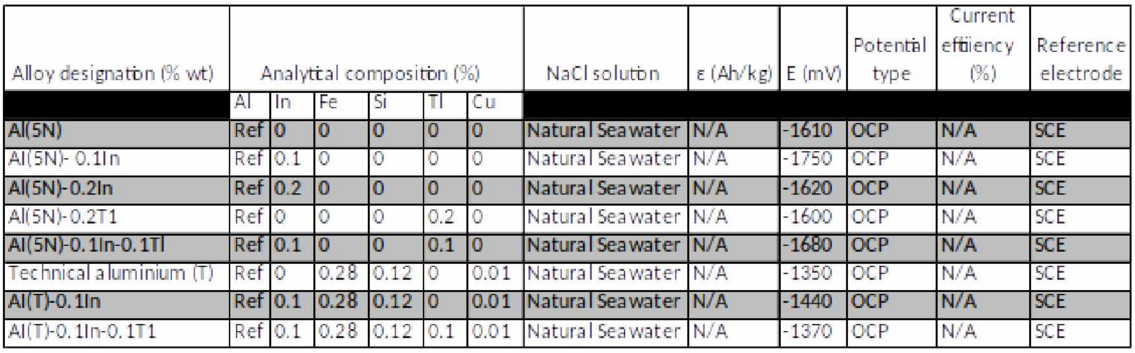

Alloy designation (% wt)	Analytical composition (%)						NaCl solution	ε (Ah/kg)	E (mV)	Potential type	Current efficiency (%)	Reference electrode
	Al	In	Fe	Si	Tl	Cu						
Al(5N)	Ref	0	0	0	0	0	Natural Seawater	N/A	-1610	OCP	N/A	SCE
Al(5N)- 0.1In	Ref	0.1	0	0	0	0	Natural Seawater	N/A	-1750	OCP	N/A	SCE
Al(5N)-0.2In	Ref	0.2	0	0	0	0	Natural Seawater	N/A	-1620	OCP	N/A	SCE
Al(5N)-0.2T1	Ref	0	0	0	0.2	0	Natural Seawater	N/A	-1600	OCP	N/A	SCE
Al(5N)-0.1In-0.1Tl	Ref	0.1	0	0	0.1	0	Natural Seawater	N/A	-1680	OCP	N/A	SCE
Technical aluminium (T)	Ref	0	0.28	0.12	0	0.01	Natural Seawater	N/A	-1350	OCP	N/A	SCE
Al(T)-0.1In	Ref	0.1	0.28	0.12	0	0.01	Natural Seawater	N/A	-1440	OCP	N/A	SCE
Al(T)-0.1In-0.1T1	Ref	0.1	0.28	0.12	0.1	0.01	Natural Seawater	N/A	-1370	OCP	N/A	SCE

Xia et al ((Xia et al.))investigated the effect of Sn, Cd and Si additions in a baseline Al-Zn-In anode. The additions were proven to be effective depassivators, leading to a uniform surface corrosion and improved electrochemical properties, compared to the baseline Al-Zn-In anode.

Table 4.11: Electrochemical performance of experimental compositions – Xia et al ((Xia et al.)).

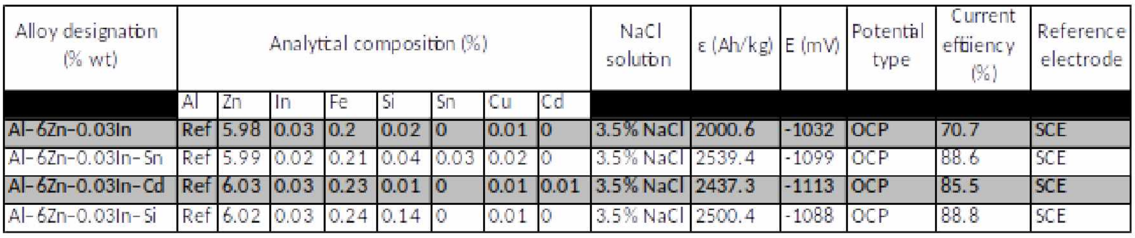

Alloy designation (% wt)	Analytical composition (%)								NaCl solution	ε (Ah/kg)	E (mV)	Potential type	Current efficiency (%)	Reference electrode
	Al	Zn	In	Fe	Si	Sn	Cu	Cd						
Al-6Zn-0.03In	Ref	5.98	0.03	0.2	0.02	0	0.01	0	3.5% NaCl	2000.6	-1032	OCP	70.7	SCE
Al-6Zn-0.03In-Sn	Ref	5.99	0.02	0.21	0.04	0.03	0.02	0	3.5% NaCl	2539.4	-1099	OCP	88.6	SCE
Al-6Zn-0.03In-Cd	Ref	6.03	0.03	0.23	0.01	0	0.01	0.01	3.5% NaCl	2437.3	-1113	OCP	85.5	SCE
Al-6Zn-0.03In-Si	Ref	6.02	0.03	0.24	0.14	0	0.01	0	3.5% NaCl	2500.4	-1088	OCP	88.8	SCE

Pourgharibshahi and Meratian ((Pourgharibshahi and Meratian, 2014)) created and tested the effects of Si, Ca and Mg additions in a baseline Al-Zn-In anode. The alloy containing Mg-Ca (Alloy IV) exhibited high electrochemical performance, but its non-uniform corrosion renders it not suitable for commercial application. The addition of Si (in alloy V) resolved the non-uniform corrosion issue, without significant penalty in current capacity. As a result, alloy V satisfies the criteria for commercial application.

Table 4.12: Electrochemical performance of experimental compositions – Pourgharibshahi et al ((Pourgharibshahi and Meratian, 2014)).

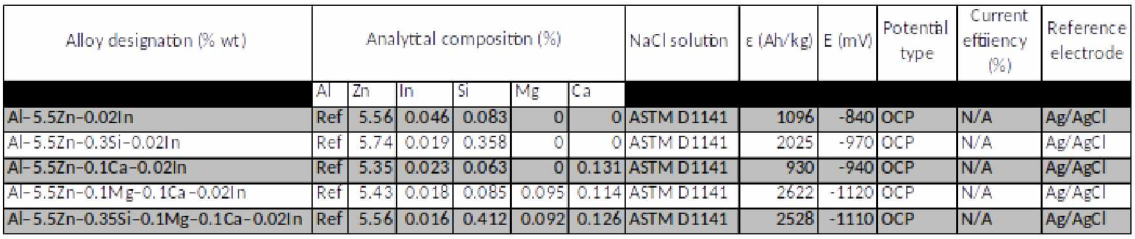

Alloy designation (% wt)	Analytical composition (%)						NaCl solution	ε (Ah/kg)	E (mV)	Potential type	Current efficiency (%)	Reference electrode
	Al	Zn	In	Si	Mg	Ca						
Al-5.5Zn-0.02In	Ref	5.56	0.046	0.083	0	0	ASTM D1141	1096	-840	OCP	N/A	Ag/AgCl
Al-5.5Zn-0.3Si-0.02In	Ref	5.74	0.019	0.358	0	0	ASTM D1141	2025	-970	OCP	N/A	Ag/AgCl
Al-5.5Zn-0.1Ca-0.02In	Ref	5.35	0.023	0.063	0	0.131	ASTM D1141	930	-940	OCP	N/A	Ag/AgCl
Al-5.5Zn-0.1Mg-0.1Ca-0.02In	Ref	5.43	0.018	0.085	0.095	0.114	ASTM D1141	2622	-1120	OCP	N/A	Ag/AgCl
Al-5.5Zn-0.35Si-0.1Mg-0.1Ca-0.02In	Ref	5.56	0.016	0.412	0.092	0.126	ASTM D1141	2528	-1110	OCP	N/A	Ag/AgCl

Farooq et al ((Farooq et al., 2019)) performed electrochemical measurements on an Al-Zn alloy created in their laboratory. The performance of the Al-Zn alloy is compared to anode compositions acquired from literature.

Barbucci et al ((Barbucci et al., 1997)) studied the corrosion behavior of three distinct Al-Zn-Mg alloys with varying annealing times and cooling methods. The morphology of the samples showed two distinct phases, phase α consisting of Aluminum (solid solution) and a secondary phase τ. The presence of these two phases as well as their volume fraction influences the activation of the anodes, with good electrochemical efficiency been attributed to good dispersion of τ phase.

Table 4.13: Electrochemical performance of experimental compositions – Farooq et al ((Farooq et al., 2019)) / Table A.

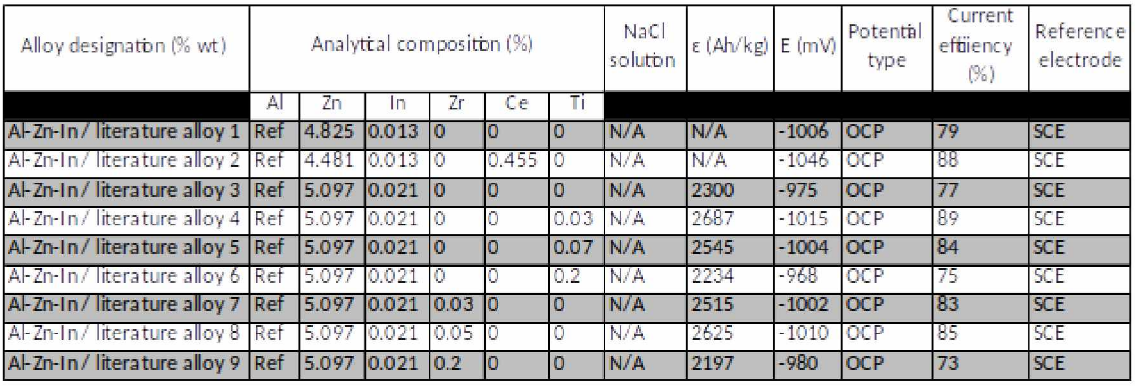

Alloy designation (% wt)	Analytical composition (%)						NaCl solution	ε (Ah/kg)	E (mV)	Potential type	Current efficiency (%)	Reference electrode
	Al	Zn	In	Zr	Ce	Ti						
Al-Zn-In / literature alloy 1	Ref	4.825	0.013	0	0	0	N/A	N/A	-1006	OCP	79	SCE
Al-Zn-In / literature alloy 2	Ref	4.481	0.013	0	0.455	0	N/A	N/A	-1046	OCP	88	SCE
Al-Zn-In / literature alloy 3	Ref	5.097	0.021	0	0	0	N/A	2300	-975	OCP	77	SCE
Al-Zn-In / literature alloy 4	Ref	5.097	0.021	0	0	0.03	N/A	2687	-1015	OCP	89	SCE
Al-Zn-In / literature alloy 5	Ref	5.097	0.021	0	0	0.07	N/A	2545	-1004	OCP	84	SCE
Al-Zn-In / literature alloy 6	Ref	5.097	0.021	0	0	0.2	N/A	2234	-968	OCP	75	SCE
Al-Zn-In / literature alloy 7	Ref	5.097	0.021	0.03	0	0	N/A	2515	-1002	OCP	83	SCE
Al-Zn-In / literature alloy 8	Ref	5.097	0.021	0.05	0	0	N/A	2625	-1010	OCP	85	SCE
Al-Zn-In / literature alloy 9	Ref	5.097	0.021	0.2	0	0	N/A	2197	-980	OCP	73	SCE

Table 4.14: Electrochemical performance of experimental compositions – Farooq et al ((Farooq et al., 2019)) / Table B.

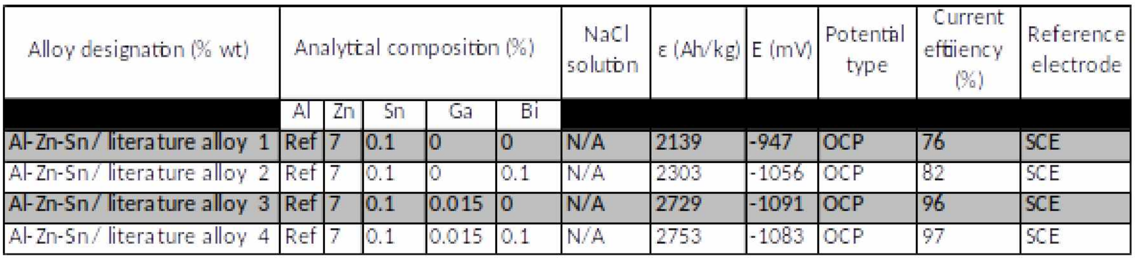

Alloy designation (% wt)	Analytical composition (%)					NaCl solution	ε (Ah/kg)	E (mV)	Potential type	Current efficiency (%)	Reference electrode
	Al	Zn	Sn	Ga	Bi						
Al-Zn-Sn / literature alloy 1	Ref	7	0.1	0	0	N/A	2139	-947	OCP	76	SCE
Al-Zn-Sn / literature alloy 2	Ref	7	0.1	0	0.1	N/A	2303	-1056	OCP	82	SCE
Al-Zn-Sn / literature alloy 3	Ref	7	0.1	0.015	0	N/A	2729	-1091	OCP	96	SCE
Al-Zn-Sn / literature alloy 4	Ref	7	0.1	0.015	0.1	N/A	2753	-1083	OCP	97	SCE

Table 4.15: Electrochemical performance of experimental compositions – Farooq et al ((Farooq et al., 2019)) / Table C.

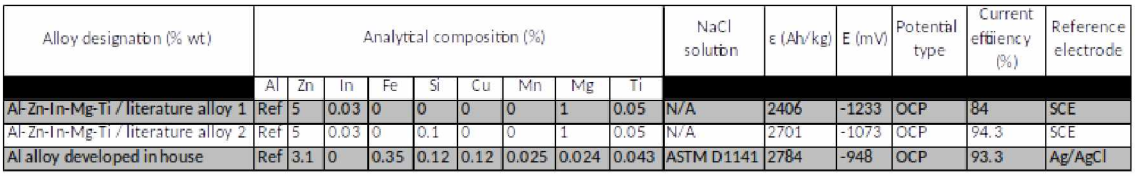

Alloy designation (% wt)	Analytical composition (%)									NaCl solution	ε (Ah/kg)	E (mV)	Potential type	Current efficiency (%)	Reference electrode
	Al	Zn	In	Fe	Si	Cu	Mn	Mg	Ti						
Al-Zn-In-Mg-Ti / literature alloy 1	Ref	5	0.03	0	0	0	0	1	0.05	N/A	2406	-1233	OCP	84	SCE
Al-Zn-In-Mg-Ti / literature alloy 2	Ref	5	0.03	0	0.1	0	0	1	0.05	N/A	2701	-1073	OCP	94.3	SCE
Al alloy developed in house	Ref	3.1	0	0.35	0.12	0.12	0.025	0.024	0.043	ASTM D1141	2784	-948	OCP	93.3	Ag/AgCl

Bruzzone et al ((Bruzzone et al., 1997)) investigated the effect of Calcium addition in Al-In and Al-Zn anodes. Ca proved to be an effective depassivator of aluminum.

He et al ((He et al., 2011)) investigated the influence of precipitates on the performance of Al-5Zn–0.03In–1Mg–0.05Ti–0.14Si. All samples were solution treated at 470 ^{o}C for one hour and afterwards subjected to individual aging treatments. The characteristics of the precipitates in the alloy (shape and size) influence the electrochemical performance of the anodes. Specifically, spherical/disk like precipitates and precipitates with moderate size were beneficial, while rod like precipitates or small size precipitates were detrimental to the anode's performance.

Table 4.16: Electrochemical performance of experimental compositions – Barbucci et al ((Barbucci et al., 1997)).

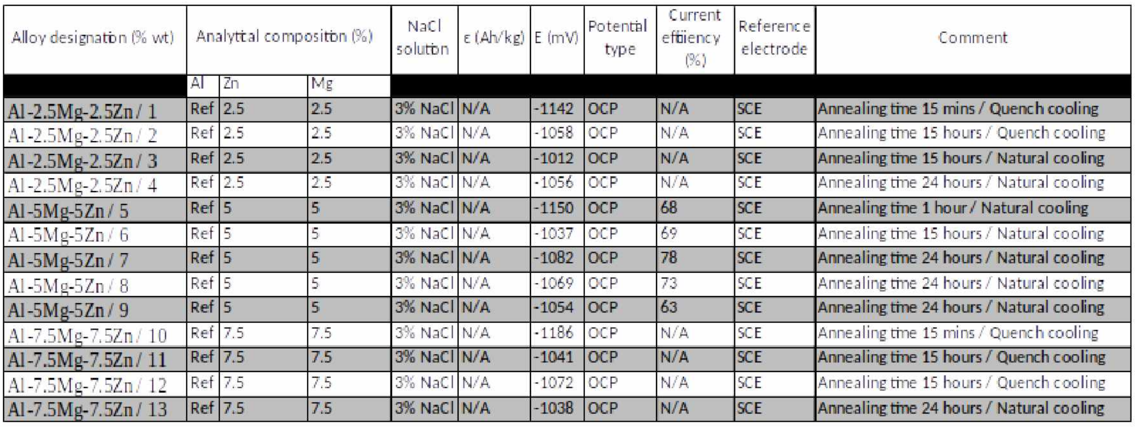

Alloy designation (% wt)	Analytical composition (%)			NaCl solution	ε (Ah/kg)	E (mV)	Potential type	Current efficiency (%)	Reference electrode	Comment
	Al	Zn	Mg							
Al-2.5Mg-2.5Zn / 1	Ref	2.5	2.5	3% NaCl	N/A	-1142	OCP	N/A	SCE	Annealing time 15 mins / Quench cooling
Al-2.5Mg-2.5Zn / 2	Ref	2.5	2.5	3% NaCl	N/A	-1058	OCP	N/A	SCE	Annealing time 15 hours / Quench cooling
Al-2.5Mg-2.5Zn / 3	Ref	2.5	2.5	3% NaCl	N/A	-1012	OCP	N/A	SCE	Annealing time 15 hours / Natural cooling
Al-2.5Mg-2.5Zn / 4	Ref	2.5	2.5	3% NaCl	N/A	-1056	OCP	N/A	SCE	Annealing time 24 hours / Natural cooling
Al-5Mg-5Zn / 5	Ref	5	5	3% NaCl	N/A	-1150	OCP	68	SCE	Annealing time 1 hour / Natural cooling
Al-5Mg-5Zn / 6	Ref	5	5	3% NaCl	N/A	-1037	OCP	69	SCE	Annealing time 15 hours / Natural cooling
Al-5Mg-5Zn / 7	Ref	5	5	3% NaCl	N/A	-1082	OCP	78	SCE	Annealing time 24 hours / Natural cooling
Al-5Mg-5Zn / 8	Ref	5	5	3% NaCl	N/A	-1069	OCP	73	SCE	Annealing time 24 hours / Natural cooling
Al-5Mg-5Zn / 9	Ref	5	5	3% NaCl	N/A	-1054	OCP	63	SCE	Annealing time 24 hours / Natural cooling
Al-7.5Mg-7.5Zn / 10	Ref	7.5	7.5	3% NaCl	N/A	-1186	OCP	N/A	SCE	Annealing time 15 mins / Quench cooling
Al-7.5Mg-7.5Zn / 11	Ref	7.5	7.5	3% NaCl	N/A	-1041	OCP	N/A	SCE	Annealing time 15 hours / Quench cooling
Al-7.5Mg-7.5Zn / 12	Ref	7.5	7.5	3% NaCl	N/A	-1072	OCP	N/A	SCE	Annealing time 15 hours / Quench cooling
Al-7.5Mg-7.5Zn / 13	Ref	7.5	7.5	3% NaCl	N/A	-1038	OCP	N/A	SCE	Annealing time 24 hours / Natural cooling

Table 4.17: Electrochemical performance of experimental compositions – Bruzzone et al ((Bruzzone et al., 1997)).

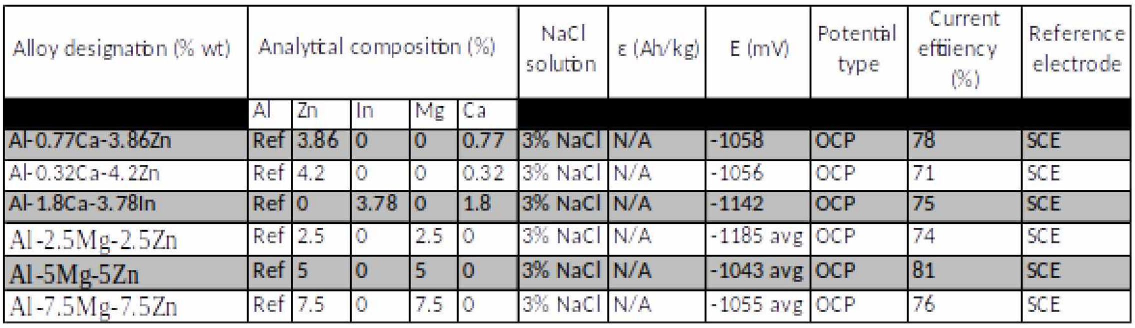

Alloy designation (% wt)	Analytical composition (%)					NaCl solution	ε (Ah/kg)	E (mV)	Potential type	Current efficiency (%)	Reference electrode
	Al	Zn	In	Mg	Ca						
Al-0.77Ca-3.86Zn	Ref	3.86	0	0	0.77	3% NaCl	N/A	-1058	OCP	78	SCE
Al-0.32Ca-4.2Zn	Ref	4.2	0	0	0.32	3% NaCl	N/A	-1056	OCP	71	SCE
Al-1.8Ca-3.78In	Ref	0	3.78	0	1.8	3% NaCl	N/A	-1142	OCP	75	SCE
Al-2.5Mg-2.5Zn	Ref	2.5	0	2.5	0	3% NaCl	N/A	-1185 avg	OCP	74	SCE
Al-5Mg-5Zn	Ref	5	0	5	0	3% NaCl	N/A	-1043 avg	OCP	81	SCE
Al-7.5Mg-7.5Zn	Ref	7.5	0	7.5	0	3% NaCl	N/A	-1055 avg	OCP	76	SCE

Table 4.18: Electrochemical performance of experimental compositions – He et al ((He et al., 2011)).

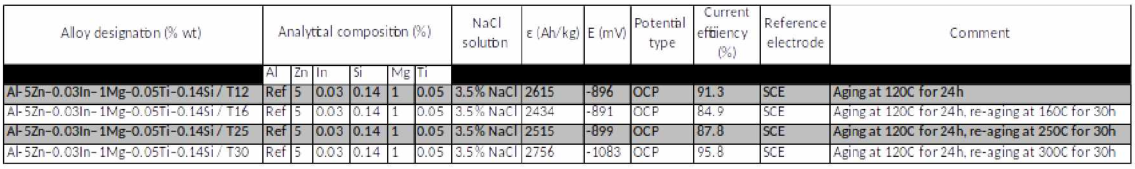

Alloy designation (% wt)	Analytical composition (%)						NaCl solution	ε (Ah/kg)	E (mV)	Potential type	Current efficiency (%)	Reference electrode	Comment
	Al	Zn	In	Si	Mg	Ti							
Al-5Zn-0.03In-1Mg-0.05Ti-0.14Si / T12	Ref	5	0.03	0.14	1	0.05	3.5% NaCl	2615	-896	OCP	91.3	SCE	Aging at 120C for 24h
Al-5Zn-0.03In-1Mg-0.05Ti-0.14Si / T16	Ref	5	0.03	0.14	1	0.05	3.5% NaCl	2434	-891	OCP	84.9	SCE	Aging at 120C for 24h, re-aging at 160C for 30h
Al-5Zn-0.03In-1Mg-0.05Ti-0.14Si / T25	Ref	5	0.03	0.14	1	0.05	3.5% NaCl	2515	-899	OCP	87.8	SCE	Aging at 120C for 24h, re-aging at 250C for 30h
Al-5Zn-0.03In-1Mg-0.05Ti-0.14Si / T30	Ref	5	0.03	0.14	1	0.05	3.5% NaCl	2756	-1083	OCP	95.8	SCE	Aging at 120C for 24h, re-aging at 300C for 30h

Ma and Wen ((Ma and Wen, 2009)) experimented with additions of Lanthanum to improve the non-uniform corrosion of a baseline Al-Zn-In-Mg-Ti alloy. Out of the four samples tested, the alloy containing 0.5wt% La exhibits high current capacity and efficiency, as well as more uniform corrosion.

Wen et al ((Wen et al., 2011)) investigated the effect of Silicon addition on the corrosion behavior of a baseline Al-Zn-In-Mg-Ti alloy. Two alloys were prepared, one with the addition of Si and one without Si for comparison purposes. The addition of silicon improved the microstructure, electrochemical performance and corrosion behavior of the

Table 4.19: Electrochemical performance of experimental compositions – Ma and Wen ((Ma and Wen, 2009)).

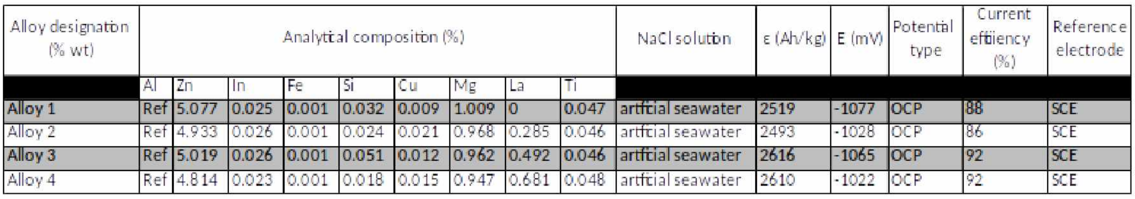

Alloy designation (% wt)	Analytical composition (%)									NaCl solution	ε (Ah/kg)	E (mV)	Potential type	Current efficiency (%)	Reference electrode
	Al	Zn	In	Fe	Si	Cu	Mg	La	Ti						
Alloy 1	**Ref**	**5.077**	**0.025**	**0.001**	**0.032**	**0.009**	**1.009**	**0**	**0.047**	**artificial seawater**	**2519**	**-1077**	**OCP**	**88**	**SCE**
Alloy 2	Ref	4.933	0.026	0.001	0.024	0.021	0.968	0.285	0.046	artificial seawater	2493	-1028	OCP	86	SCE
Alloy 3	**Ref**	**5.019**	**0.026**	**0.001**	**0.051**	**0.012**	**0.962**	**0.492**	**0.046**	**artificial seawater**	**2616**	**-1065**	**OCP**	**92**	**SCE**
Alloy 4	Ref	4.814	0.023	0.001	0.018	0.015	0.947	0.681	0.048	artificial seawater	2610	-1022	OCP	92	SCE

alloy. The Open Circuit Potential took more positive values, closer to the ideal range for protection of iron in seawater.

Table 4.20: Electrochemical performance of experimental compositions – Wen et al ((Wen et al., 2011)).

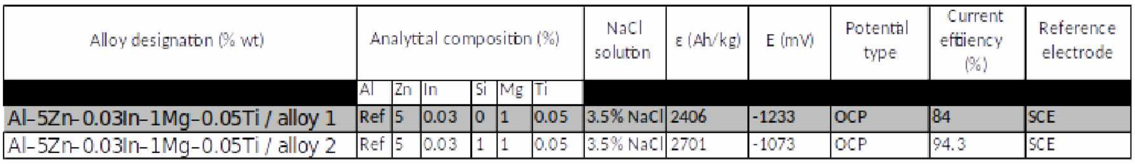

Alloy designation (% wt)	Analytical composition (%)						NaCl solution	ε (Ah/kg)	E (mV)	Potential type	Current efficiency (%)	Reference electrode
	Al	Zn	In	Si	Mg	Ti						
Al-5Zn-0.03In-1Mg-0.05Ti / alloy 1	**Ref**	**5**	**0.03**	**0**	**1**	**0.05**	**3.5% NaCl**	**2406**	**-1233**	**OCP**	**84**	**SCE**
Al-5Zn-0.03In-1Mg-0.05Ti / alloy 2	Ref	5	0.03	1	1	0.05	3.5% NaCl	2701	-1073	OCP	94.3	SCE

Ma and Wen ((Ma and Wen, 2010)) studied the corrosion behavior of an Al-Zn-In-Mg-Ti-Mn alloy. The corrosion of the alloy was attributed to mechanisms that varied with immersion time. Specifically, at the initial stages of immersion the prevalent corrosion mechanism was pitting corrosion. Afterwards, a dissolution-precipitation mechanism of In and Zn ions is observed and finally a uniform corrosion of the anode's surface was observed. Similar findings were observed from Ma et al ((Ma et al., 2012)) in the corrosion behavior study of an Al-Zn-In-Mg-Ti-Ce alloy, as the initial pitting corrosion subsided with time and a dissolution-precipitation mechanism became the prevalent one.

Table 4.21: Electrochemical performance of experimental compositions – Ma and Wen ((Ma and Wen, 2010)).

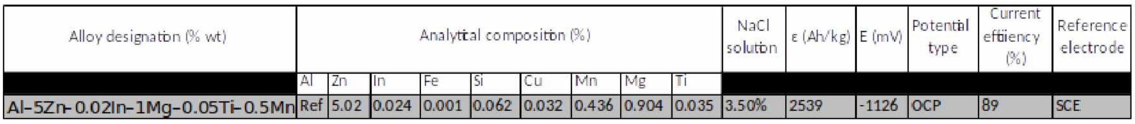

Alloy designation (% wt)	Analytical composition (%)									NaCl solution	ε (Ah/kg)	E (mV)	Potential type	Current efficiency (%)	Reference electrode
	Al	Zn	In	Fe	Si	Cu	Mn	Mg	Ti						
Al-5Zn-0.02In-1Mg-0.05Ti-0.5Mn	Ref	5.02	0.024	0.001	0.062	0.032	0.436	0.904	0.035	3.50%	2539	-1126	OCP	89	SCE

Saeri and Keyvani ((Saeri and Keyvani, 2011)) studied the effects of Magnesium and Manganese additions on the performance of an Al-Zn-In baseline alloy. Additions of both elements are beneficial up to a specific concentration, specifically Mn addition up to 0.15wt% and Mg addition up to 2wt%.

Table 4.22: Electrochemical performance of experimental compositions – Ma et al ((Ma et al., 2012)).

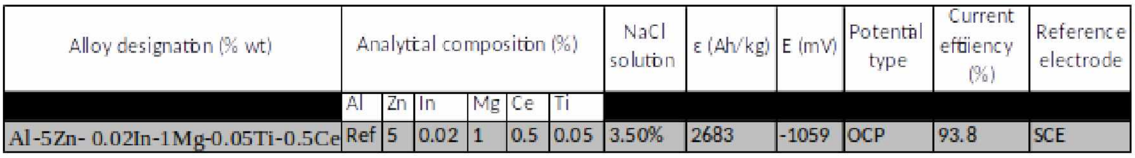

Alloy designation (% wt)	Analytical composition (%)						NaCl solution	ε (Ah/kg)	E (mV)	Potential type	Current efficiency (%)	Reference electrode
	Al	Zn	In	Mg	Ce	Ti						
Al-5Zn- 0.02In-1Mg-0.05Ti-0.5Ce	Ref	5	0.02	1	0.5	0.05	3.50%	2683	-1059	OCP	93.8	SCE

Table 4.23: Electrochemical performance of experimental compositions – Saeri et al ((Saeri and Keyvani, 2011)) / Table A.

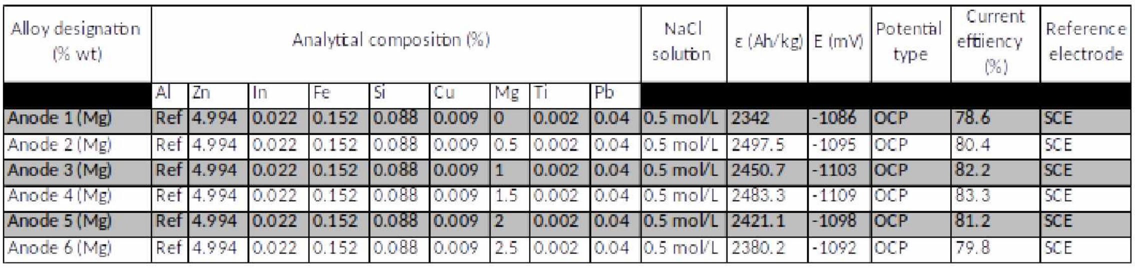

Alloy designation (% wt)	Analytical composition (%)									NaCl solution	ε (Ah/kg)	E (mV)	Potential type	Current efficiency (%)	Reference electrode
	Al	Zn	In	Fe	Si	Cu	Mg	Ti	Pb						
Anode 1 (Mg)	Ref	4.994	0.022	0.152	0.088	0.009	0	0.002	0.04	0.5 mol/L	2342	-1086	OCP	78.6	SCE
Anode 2 (Mg)	Ref	4.994	0.022	0.152	0.088	0.009	0.5	0.002	0.04	0.5 mol/L	2497.5	-1095	OCP	80.4	SCE
Anode 3 (Mg)	Ref	4.994	0.022	0.152	0.088	0.009	1	0.002	0.04	0.5 mol/L	2450.7	-1103	OCP	82.2	SCE
Anode 4 (Mg)	Ref	4.994	0.022	0.152	0.088	0.009	1.5	0.002	0.04	0.5 mol/L	2483.3	-1109	OCP	83.3	SCE
Anode 5 (Mg)	Ref	4.994	0.022	0.152	0.088	0.009	2	0.002	0.04	0.5 mol/L	2421.1	-1098	OCP	81.2	SCE
Anode 6 (Mg)	Ref	4.994	0.022	0.152	0.088	0.009	2.5	0.002	0.04	0.5 mol/L	2380.2	-1092	OCP	79.8	SCE

Table 4.24: Electrochemical performance of experimental compositions – Saeri et al ((Saeri and Keyvani, 2011)) / Table B.

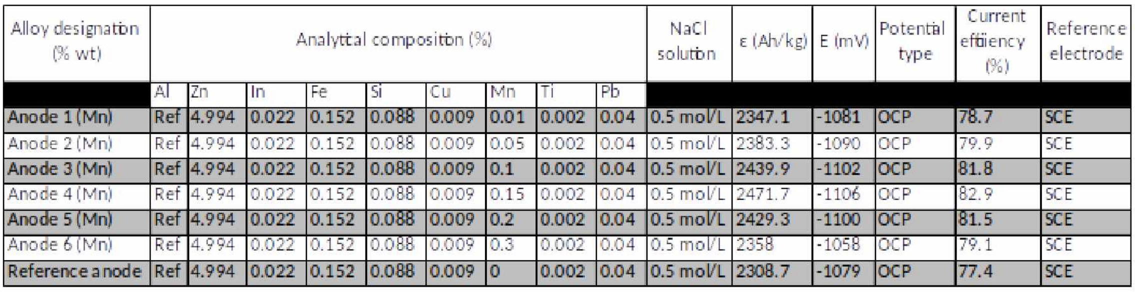

Alloy designation (% wt)	Analytical composition (%)									NaCl solution	ε (Ah/kg)	E (mV)	Potential type	Current efficiency (%)	Reference electrode
	Al	Zn	In	Fe	Si	Cu	Mn	Ti	Pb						
Anode 1 (Mn)	Ref	4.994	0.022	0.152	0.088	0.009	0.01	0.002	0.04	0.5 mol/L	2347.1	-1081	OCP	78.7	SCE
Anode 2 (Mn)	Ref	4.994	0.022	0.152	0.088	0.009	0.05	0.002	0.04	0.5 mol/L	2383.3	-1090	OCP	79.9	SCE
Anode 3 (Mn)	Ref	4.994	0.022	0.152	0.088	0.009	0.1	0.002	0.04	0.5 mol/L	2439.9	-1102	OCP	81.8	SCE
Anode 4 (Mn)	Ref	4.994	0.022	0.152	0.088	0.009	0.15	0.002	0.04	0.5 mol/L	2471.7	-1106	OCP	82.9	SCE
Anode 5 (Mn)	Ref	4.994	0.022	0.152	0.088	0.009	0.2	0.002	0.04	0.5 mol/L	2429.3	-1100	OCP	81.5	SCE
Anode 6 (Mn)	Ref	4.994	0.022	0.152	0.088	0.009	0.3	0.002	0.04	0.5 mol/L	2358	-1058	OCP	79.1	SCE
Reference anode	Ref	4.994	0.022	0.152	0.088	0.009	0	0.002	0.04	0.5 mol/L	2308.7	-1079	OCP	77.4	SCE

Shibli et al ((Shibli et al., 2004)) explored the possibility of Al-Zn alloy activation with the use of ruthenium dioxide coatings. First, tests were conducted with firing temperatures ranging from 300 ^oC to 1500 ^oC, followed by tests with varying surface concentrations of RuO_2. The final test was comprised of the optimum surface RuO_2 concentrations, varying temperatures, and a mild stirring of the solution to simulate water flow. The ruthenium oxide covered surface was conductive, catalytically active and yielded promising results under full activation.

A similar research, conducted by Shibli and Gireesh ((Shibli and Gireesh, 2003)) explored the possibility of Al-Zn alloy activation with the use of iridium dioxide coatings. The IrO_2 covered surface was conductive, catalytically active and yielded promising results for coating concentrations greater than 0.175mg/cm2.

Table 4.25: Electrochemical performance of experimental compositions – Shibli et al ((Shibli et al., 2004)).

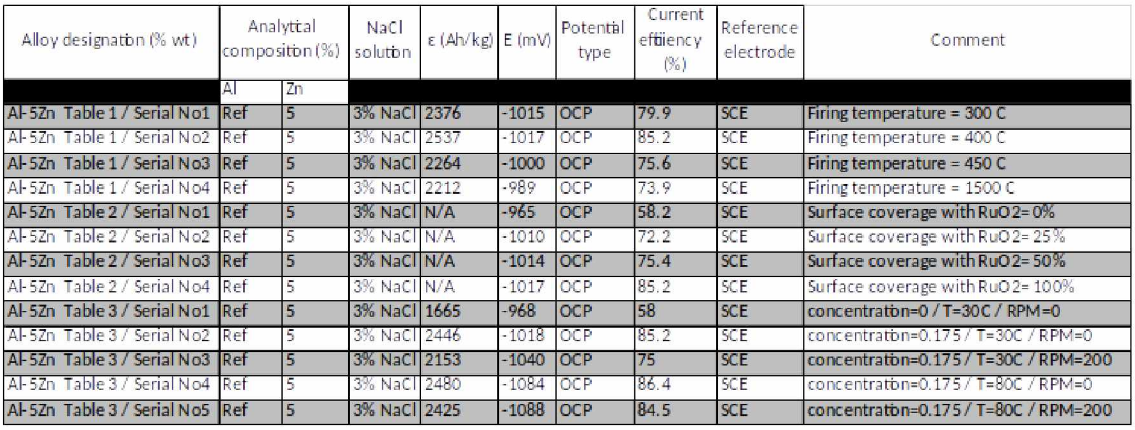

Alloy designation (% wt)	Analytical composition (%)		NaCl solution	ε (Ah/kg)	E (mV)	Potential type	Current efficiency (%)	Reference electrode	Comment
	Al	Zn							
Al-5Zn Table 1 / Serial No1	Ref	5	3% NaCl	2376	-1015	OCP	79.9	SCE	Firing temperature = 300 C
Al-5Zn Table 1 / Serial No2	Ref	5	3% NaCl	2537	-1017	OCP	85.2	SCE	Firing temperature = 400 C
Al-5Zn Table 1 / Serial No3	Ref	5	3% NaCl	2264	-1000	OCP	75.6	SCE	Firing temperature = 450 C
Al-5Zn Table 1 / Serial No4	Ref	5	3% NaCl	2212	-989	OCP	73.9	SCE	Firing temperature = 1500 C
Al-5Zn Table 2 / Serial No1	Ref	5	3% NaCl	N/A	-965	OCP	58.2	SCE	Surface coverage with RuO2= 0%
Al-5Zn Table 2 / Serial No2	Ref	5	3% NaCl	N/A	-1010	OCP	72.2	SCE	Surface coverage with RuO2= 25%
Al-5Zn Table 2 / Serial No3	Ref	5	3% NaCl	N/A	-1014	OCP	75.4	SCE	Surface coverage with RuO2= 50%
Al-5Zn Table 2 / Serial No4	Ref	5	3% NaCl	N/A	-1017	OCP	85.2	SCE	Surface coverage with RuO2= 100%
Al-5Zn Table 3 / Serial No1	Ref	5	3% NaCl	1665	-968	OCP	58	SCE	concentration=0 / T=30C / RPM=0
Al-5Zn Table 3 / Serial No2	Ref	5	3% NaCl	2446	-1018	OCP	85.2	SCE	concentration=0.175 / T=30C / RPM=0
Al-5Zn Table 3 / Serial No3	Ref	5	3% NaCl	2153	-1040	OCP	75	SCE	concentration=0.175 / T=30C / RPM=200
Al-5Zn Table 3 / Serial No4	Ref	5	3% NaCl	2480	-1084	OCP	86.4	SCE	concentration=0.175 / T=80C / RPM=0
Al-5Zn Table 3 / Serial No5	Ref	5	3% NaCl	2425	-1088	OCP	84.5	SCE	concentration=0.175 / T=80C / RPM=200

Table 4.26: Electrochemical performance of experimental compositions – Shibli and Gireesh((Shibli and Gireesh, 2003)).

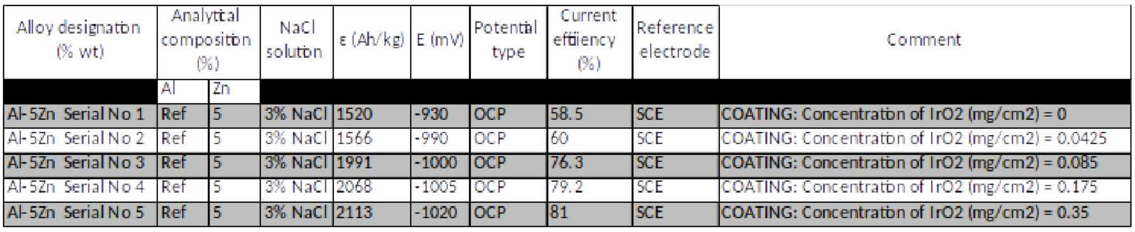

Alloy designation (% wt)	Analytical composition (%)		NaCl solution	ε (Ah/kg)	E (mV)	Potential type	Current efficiency (%)	Reference electrode	Comment
	Al	Zn							
Al-5Zn Serial No 1	Ref	5	3% NaCl	1520	-930	OCP	58.5	SCE	COATING: Concentration of IrO2 (mg/cm2) = 0
Al-5Zn Serial No 2	Ref	5	3% NaCl	1566	-990	OCP	60	SCE	COATING: Concentration of IrO2 (mg/cm2) = 0.0425
Al-5Zn Serial No 3	Ref	5	3% NaCl	1991	-1000	OCP	76.3	SCE	COATING: Concentration of IrO2 (mg/cm2) = 0.085
Al-5Zn Serial No 4	Ref	5	3% NaCl	2068	-1005	OCP	79.2	SCE	COATING: Concentration of IrO2 (mg/cm2) = 0.175
Al-5Zn Serial No 5	Ref	5	3% NaCl	2113	-1020	OCP	81	SCE	COATING: Concentration of IrO2 (mg/cm2) = 0.35

Shibli et al ((Shibli et al., 2007)) continued to experiment with metal oxides, in the form of alumina (Al_2O_3) and zinc oxide (ZnO) additions to baseline Al-Zn sacrificial anode alloys. The addition of ZnO improved the metallurgical structure and the galvanic characteristics during exposure, resulting in improved performance and corrosion behavior. On the other hand, the addition of alumina had no significant influence on the metallurgical structure and electrochemical performance of the anodes, mainly due to the "seeding" of Al_2O_3 in the oxide layer of the anode. The ZnO particles are promising additions and the combination of zinc oxide with elements such as Indium could yield even better performance.

Shibli and Gireesh ((Shibli and Gireesh, 2005)) studied the effect of selenium addition to a baseline Al-Zn and Al-Zn-Bi-Sn alloys. Small additions of Se (0.5wt%) as sole alloying addition improved the metallographic structure of the anode. The best performing composition was found to be the Al-5Zn-0.1Sn-0.1Se-0.1Bi, a result that is in line with the uniform corrosion behavior of the alloy.

Table 4.27: Electrochemical performance of experimental compositions – Shibli et al ((Shibli et al., 2007)).

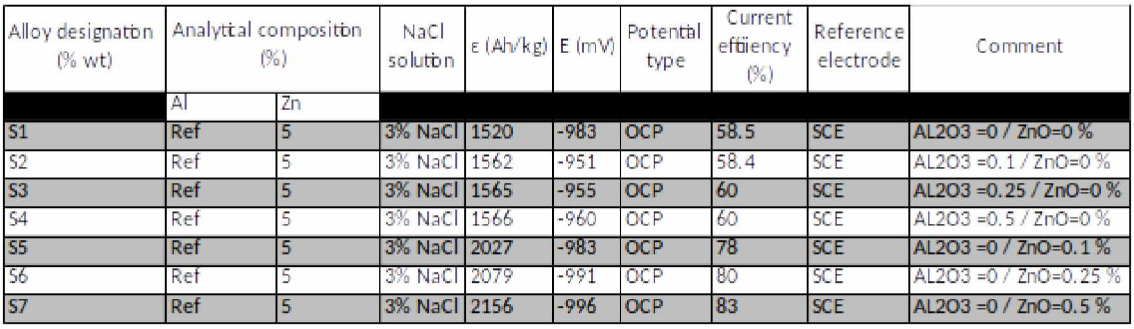

Alloy designation (% wt)	Analytical composition (%)		NaCl solution	ε (Ah/kg)	E (mV)	Potential type	Current efficiency (%)	Reference electrode	Comment
	Al	Zn							
S1	Ref	5	3% NaCl	1520	-983	OCP	58.5	SCE	AL2O3 =0 / ZnO=0 %
S2	Ref	5	3% NaCl	1562	-951	OCP	58.4	SCE	AL2O3 =0.1 / ZnO=0 %
S3	Ref	5	3% NaCl	1565	-955	OCP	60	SCE	AL2O3 =0.25 / ZnO=0 %
S4	Ref	5	3% NaCl	1566	-960	OCP	60	SCE	AL2O3 =0.5 / ZnO=0 %
S5	Ref	5	3% NaCl	2027	-983	OCP	78	SCE	AL2O3 =0 / ZnO=0.1 %
S6	Ref	5	3% NaCl	2079	-991	OCP	80	SCE	AL2O3 =0 / ZnO=0.25 %
S7	Ref	5	3% NaCl	2156	-996	OCP	83	SCE	AL2O3 =0 / ZnO=0.5 %

Table 4.28: Electrochemical performance of experimental compositions – Shibli and Gireesh ((Shibli and Gireesh, 2005)).

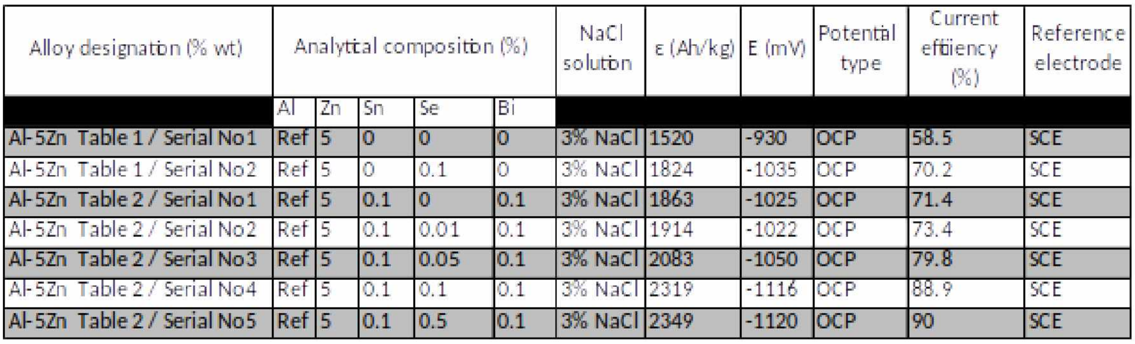

Alloy designation (% wt)	Analytical composition (%)					NaCl solution	ε (Ah/kg)	E (mV)	Potential type	Current efficiency (%)	Reference electrode
	Al	Zn	Sn	Se	Bi						
Al-5Zn Table 1 / Serial No1	Ref	5	0	0	0	3% NaCl	1520	-930	OCP	58.5	SCE
Al-5Zn Table 1 / Serial No2	Ref	5	0	0.1	0	3% NaCl	1824	-1035	OCP	70.2	SCE
Al-5Zn Table 2 / Serial No1	Ref	5	0.1	0	0.1	3% NaCl	1863	-1025	OCP	71.4	SCE
Al-5Zn Table 2 / Serial No2	Ref	5	0.1	0.01	0.1	3% NaCl	1914	-1022	OCP	73.4	SCE
Al-5Zn Table 2 / Serial No3	Ref	5	0.1	0.05	0.1	3% NaCl	2083	-1050	OCP	79.8	SCE
Al-5Zn Table 2 / Serial No4	Ref	5	0.1	0.1	0.1	3% NaCl	2319	-1116	OCP	88.9	SCE
Al-5Zn Table 2 / Serial No5	Ref	5	0.1	0.5	0.1	3% NaCl	2349	-1120	OCP	90	SCE

Shibli et al ((Shibli et al., 2008)) investigated the effect of cerium oxide on the performance characteristics and corrosion behavior of a baseline Al-Zn alloy. When CeO_2 is uniformly distributed in the anode, it effectively suppresses the formation of Al_2O_3 in the surface of the anode. A welcome side effect of Cerium oxide is the antifouling protection it offers, due to its biocidal properties.

Table 4.29: Electrochemical performance of experimental compositions – Shibli et al ((Shibli et al., 2008)).

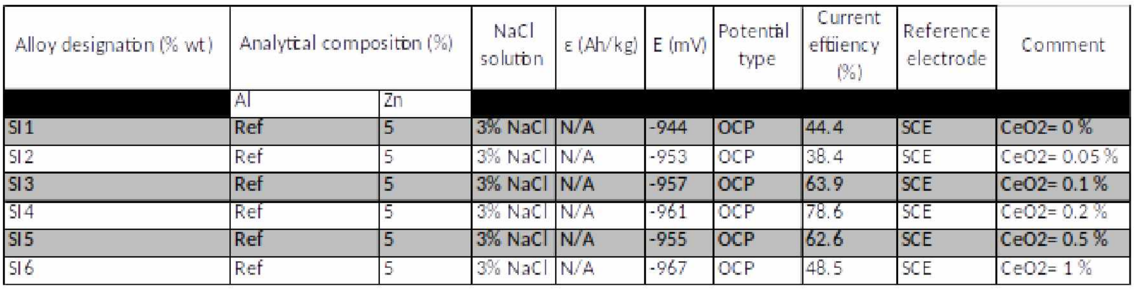

Alloy designation (% wt)	Analytical composition (%)		NaCl solution	ε (Ah/kg)	E (mV)	Potential type	Current efficiency (%)	Reference electrode	Comment
	Al	Zn							
SI1	Ref	5	3% NaCl	N/A	-944	OCP	44.4	SCE	CeO2= 0 %
SI2	Ref	5	3% NaCl	N/A	-953	OCP	38.4	SCE	CeO2= 0.05 %
SI3	Ref	5	3% NaCl	N/A	-957	OCP	63.9	SCE	CeO2= 0.1 %
SI4	Ref	5	3% NaCl	N/A	-961	OCP	78.6	SCE	CeO2= 0.2 %
SI5	Ref	5	3% NaCl	N/A	-955	OCP	62.6	SCE	CeO2= 0.5 %
SI6	Ref	5	3% NaCl	N/A	-967	OCP	48.5	SCE	CeO2= 1 %

Tsai ((Tsai, 1996)) investigated the electrochemical performance of mainstream Aluminum sacrificial anode compositions (Al-Zn-In) with variations in Zinc and Indium content. The results are satisfactory for the protection of offshore structures in seawater.

Table 4.30: Electrochemical performance of experimental compositions – Tsai ((Tsai, 1996)).

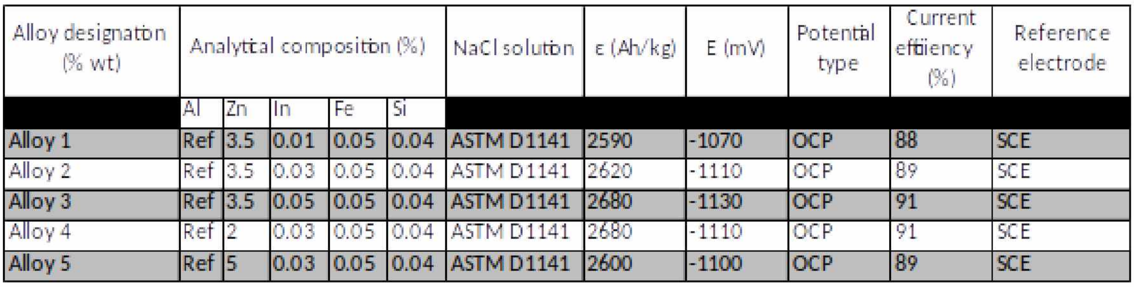

Alloy designation (% wt)	Analytical composition (%)					NaCl solution	ε (Ah/kg)	E (mV)	Potential type	Current efficiency (%)	Reference electrode
	Al	Zn	In	Fe	Si						
Alloy 1	Ref	3.5	0.01	0.05	0.04	ASTM D1141	2590	-1070	OCP	88	SCE
Alloy 2	Ref	3.5	0.03	0.05	0.04	ASTM D1141	2620	-1110	OCP	89	SCE
Alloy 3	Ref	3.5	0.05	0.05	0.04	ASTM D1141	2680	-1130	OCP	91	SCE
Alloy 4	Ref	2	0.03	0.05	0.04	ASTM D1141	2680	-1110	OCP	91	SCE
Alloy 5	Ref	5	0.03	0.05	0.04	ASTM D1141	2600	-1100	OCP	89	SCE

Ma et al ((Ma et al., 2009)) experimented with Zinc and Bismuth in an effort to create a high-performance Aluminum anode. Increased Bismuth concentrations lead to a small positive shift in potentials and improvements in the dissolution process. All anodes exhibited good electrochemical performance, but the corrosion mechanism must be researched further.

Table 4.31: Electrochemical performance of experimental compositions – Ma et al ((Ma et al., 2009)).

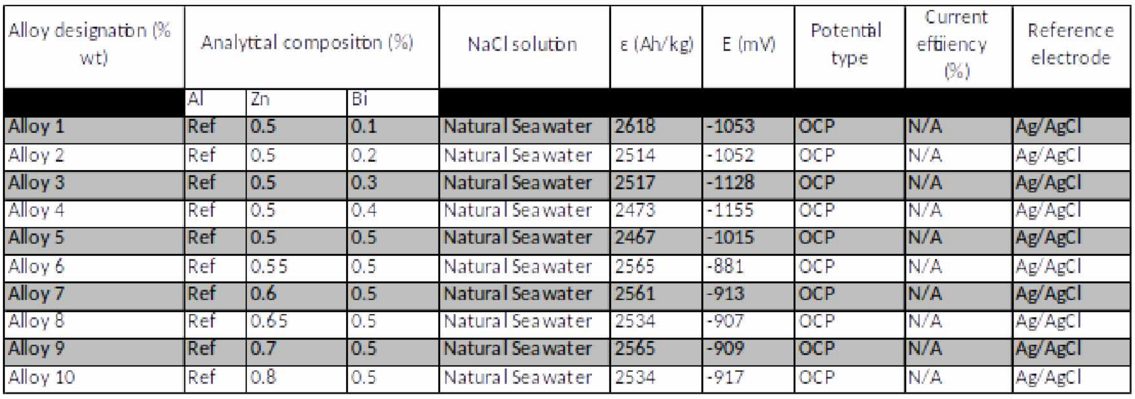

Alloy designation (% wt)	Analytical composition (%)			NaCl solution	ε (Ah/kg)	E (mV)	Potential type	Current efficiency (%)	Reference electrode
	Al	Zn	Bi						
Alloy 1	Ref	0.5	0.1	Natural Seawater	2618	-1053	OCP	N/A	Ag/AgCl
Alloy 2	Ref	0.5	0.2	Natural Seawater	2514	-1052	OCP	N/A	Ag/AgCl
Alloy 3	Ref	0.5	0.3	Natural Seawater	2517	-1128	OCP	N/A	Ag/AgCl
Alloy 4	Ref	0.5	0.4	Natural Seawater	2473	-1155	OCP	N/A	Ag/AgCl
Alloy 5	Ref	0.5	0.5	Natural Seawater	2467	-1015	OCP	N/A	Ag/AgCl
Alloy 6	Ref	0.55	0.5	Natural Seawater	2565	-881	OCP	N/A	Ag/AgCl
Alloy 7	Ref	0.6	0.5	Natural Seawater	2561	-913	OCP	N/A	Ag/AgCl
Alloy 8	Ref	0.65	0.5	Natural Seawater	2534	-907	OCP	N/A	Ag/AgCl
Alloy 9	Ref	0.7	0.5	Natural Seawater	2565	-909	OCP	N/A	Ag/AgCl
Alloy 10	Ref	0.8	0.5	Natural Seawater	2534	-917	OCP	N/A	Ag/AgCl

Saremi et al ((Saremi et al., 2004)) studied the effect of mold and melt temperature in the performance of Al-Zn-In and Al-Zn-In-Mg alloys (table for 4.1 and table for 4.2). Mold and melt temperatures as well as the solidification process are very important parameters in the even distribution of alloying elements within the anode and the resulting uniform consumption during its service life. The researchers concluded that additions of Mg lead to grain refinement in Al-Zn-In alloys, with maximum grain refinement achieved at the maximum solid solubility of Mg in Aluminum at room temperature, i.e., 2% weight. The improved grain refinement leads to layer by layer dissolution of the anode and therefore improved current capacity. ((Saremi et al., 2004))

Table 4.32: Electrochemical performance of experimental compositions – Sameri et al ((Saremi et al., 2004)) / Table A.

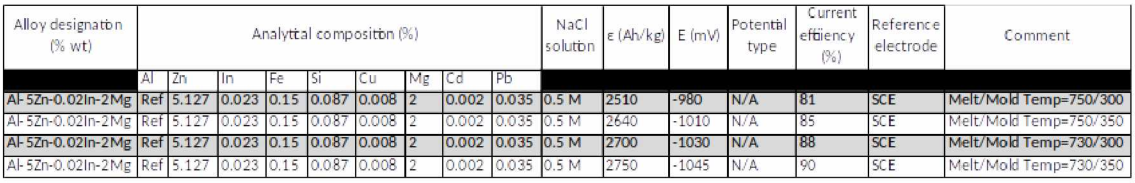

Alloy designation (% wt)	Analytical composition (%)									NaCl solution	ε (Ah/kg)	E (mV)	Potential type	Current efficiency (%)	Reference electrode	Comment
	Al	Zn	In	Fe	Si	Cu	Mg	Cd	Pb							
Al-5Zn-0.02In-2Mg	Ref	5.127	0.023	0.15	0.087	0.008	2	0.002	0.035	0.5 M	2510	-980	N/A	81	SCE	Melt/Mold Temp=750/300
Al-5Zn-0.02In-2Mg	Ref	5.127	0.023	0.15	0.087	0.008	2	0.002	0.035	0.5 M	2640	-1010	N/A	85	SCE	Melt/Mold Temp=750/350
Al-5Zn-0.02In-2Mg	Ref	5.127	0.023	0.15	0.087	0.008	2	0.002	0.035	0.5 M	2700	-1030	N/A	88	SCE	Melt/Mold Temp=730/300
Al-5Zn-0.02In-2Mg	Ref	5.127	0.023	0.15	0.087	0.008	2	0.002	0.035	0.5 M	2750	-1045	N/A	90	SCE	Melt/Mold Temp=730/350

Table 4.33: Electrochemical performance of experimental compositions – Sameri et al ((Saremi et al., 2004)) / Table B.

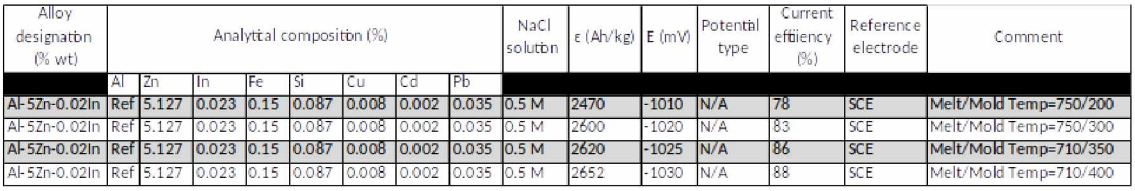

Alloy designation (% wt)	Analytical composition (%)								NaCl solution	ε (Ah/kg)	E (mV)	Potential type	Current efficiency (%)	Reference electrode	Comment
	Al	Zn	In	Fe	Si	Cu	Cd	Pb							
Al-5Zn-0.02In	Ref	5.127	0.023	0.15	0.087	0.008	0.002	0.035	0.5 M	2470	-1010	N/A	78	SCE	Melt/Mold Temp=750/200
Al-5Zn-0.02In	Ref	5.127	0.023	0.15	0.087	0.008	0.002	0.035	0.5 M	2600	-1020	N/A	83	SCE	Melt/Mold Temp=750/300
Al-5Zn-0.02In	Ref	5.127	0.023	0.15	0.087	0.008	0.002	0.035	0.5 M	2620	-1025	N/A	86	SCE	Melt/Mold Temp=710/350
Al-5Zn-0.02In	Ref	5.127	0.023	0.15	0.087	0.008	0.002	0.035	0.5 M	2652	-1030	N/A	88	SCE	Melt/Mold Temp=710/400

Keyvani et al ((Keyvani et al., 2005)) studied the effect of Casting parameters, namely melt temperature and mold temperature, in the performance and structure of Al-Zn-In anodes. The cooling rate affects greatly the performance of the resulting anode. The optimal melt temperature was found to be 710 ^oC, with a mold temperature of 400C. Generally, higher melt and mold temperatures resulted in higher electrochemical performance and uniform corrosion due to the homogeneity of alloying elements distribution within the alloy.

Sharma et al ((Sharma, 2011)) as part of their research recorder the compositions and electrochemical performance of Aluminum sacrificial anodes from various sources. The summary of their findings is presented below:

Table 4.34: Electrochemical performance of experimental compositions – Keyvani et al ((Keyvani et al., 2005)).

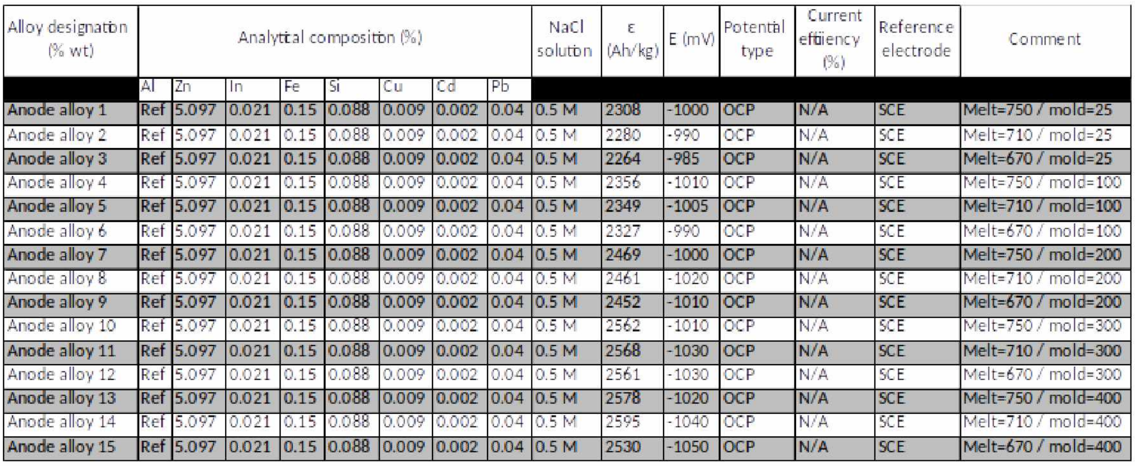

Alloy designation (% wt)	Analytical composition (%)								NaCl solution	ε (Ah/kg)	E (mV)	Potential type	Current efficiency (%)	Reference electrode	Comment
	Al	Zn	In	Fe	Si	Cu	Cd	Pb							
Anode alloy 1	Ref	5.097	0.021	0.15	0.088	0.009	0.002	0.04	0.5 M	2308	-1000	OCP	N/A	SCE	Melt=750 / mold=25
Anode alloy 2	Ref	5.097	0.021	0.15	0.088	0.009	0.002	0.04	0.5 M	2280	-990	OCP	N/A	SCE	Melt=710 / mold=25
Anode alloy 3	Ref	5.097	0.021	0.15	0.088	0.009	0.002	0.04	0.5 M	2264	-985	OCP	N/A	SCE	Melt=670 / mold=25
Anode alloy 4	Ref	5.097	0.021	0.15	0.088	0.009	0.002	0.04	0.5 M	2356	-1010	OCP	N/A	SCE	Melt=750 / mold=100
Anode alloy 5	Ref	5.097	0.021	0.15	0.088	0.009	0.002	0.04	0.5 M	2349	-1005	OCP	N/A	SCE	Melt=710 / mold=100
Anode alloy 6	Ref	5.097	0.021	0.15	0.088	0.009	0.002	0.04	0.5 M	2327	-990	OCP	N/A	SCE	Melt=670 / mold=100
Anode alloy 7	Ref	5.097	0.021	0.15	0.088	0.009	0.002	0.04	0.5 M	2469	-1000	OCP	N/A	SCE	Melt=750 / mold=200
Anode alloy 8	Ref	5.097	0.021	0.15	0.088	0.009	0.002	0.04	0.5 M	2461	-1020	OCP	N/A	SCE	Melt=710 / mold=200
Anode alloy 9	Ref	5.097	0.021	0.15	0.088	0.009	0.002	0.04	0.5 M	2452	-1010	OCP	N/A	SCE	Melt=670 / mold=200
Anode alloy 10	Ref	5.097	0.021	0.15	0.088	0.009	0.002	0.04	0.5 M	2562	-1010	OCP	N/A	SCE	Melt=750 / mold=300
Anode alloy 11	Ref	5.097	0.021	0.15	0.088	0.009	0.002	0.04	0.5 M	2568	-1030	OCP	N/A	SCE	Melt=710 / mold=300
Anode alloy 12	Ref	5.097	0.021	0.15	0.088	0.009	0.002	0.04	0.5 M	2561	-1030	OCP	N/A	SCE	Melt=670 / mold=300
Anode alloy 13	Ref	5.097	0.021	0.15	0.088	0.009	0.002	0.04	0.5 M	2578	-1020	OCP	N/A	SCE	Melt=750 / mold=400
Anode alloy 14	Ref	5.097	0.021	0.15	0.088	0.009	0.002	0.04	0.5 M	2595	-1040	OCP	N/A	SCE	Melt=710 / mold=400
Anode alloy 15	Ref	5.097	0.021	0.15	0.088	0.009	0.002	0.04	0.5 M	2530	-1050	OCP	N/A	SCE	Melt=670 / mold=400

Table 4.35: Electrochemical performance of experimental compositions – Sharma et al ((Sharma, 2011)) / Table A.

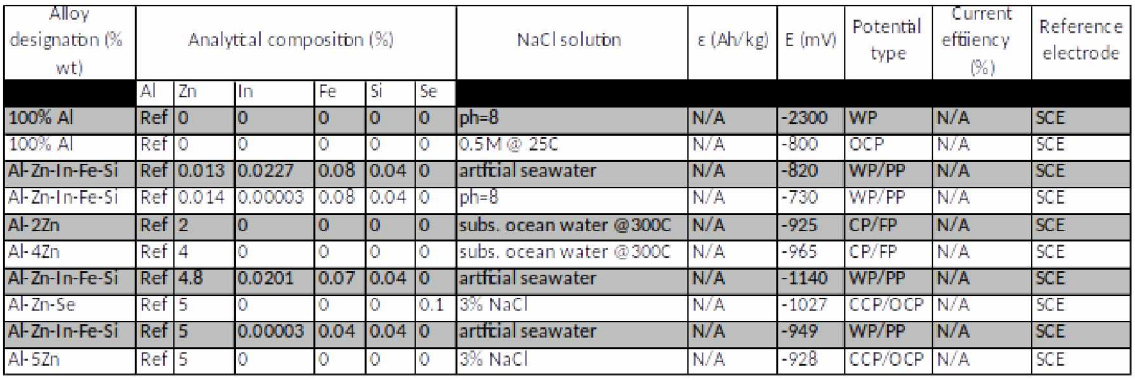

Alloy designation (% wt)	Analytical composition (%)						NaCl solution	ε (Ah/kg)	E (mV)	Potential type	Current efficiency (%)	Reference electrode
	Al	Zn	In	Fe	Si	Se						
100% Al	Ref	0	0	0	0	0	ph=8	N/A	-2300	WP	N/A	SCE
100% Al	Ref	0	0	0	0	0	0.5M @ 25C	N/A	-800	OCP	N/A	SCE
Al-Zn-In-Fe-Si	Ref	0.013	0.0227	0.08	0.04	0	artificial seawater	N/A	-820	WP/PP	N/A	SCE
Al-Zn-In-Fe-Si	Ref	0.014	0.00003	0.08	0.04	0	ph=8	N/A	-730	WP/PP	N/A	SCE
Al-2Zn	Ref	2	0	0	0	0	subs. ocean water @300C	N/A	-925	CP/FP	N/A	SCE
Al-4Zn	Ref	4	0	0	0	0	subs. ocean water @300C	N/A	-965	CP/FP	N/A	SCE
Al-Zn-In-Fe-Si	Ref	4.8	0.0201	0.07	0.04	0	artificial seawater	N/A	-1140	WP/PP	N/A	SCE
Al-Zn-Se	Ref	5	0	0	0	0.1	3% NaCl	N/A	-1027	CCP/OCP	N/A	SCE
Al-Zn-In-Fe-Si	Ref	5	0.00003	0.04	0.04	0	artificial seawater	N/A	-949	WP/PP	N/A	SCE
Al-5Zn	Ref	5	0	0	0	0	3% NaCl	N/A	-928	CCP/OCP	N/A	SCE

Table 4.36: Electrochemical performance of experimental compositions – Sharma et al ((Sharma, 2011)) / Table B.

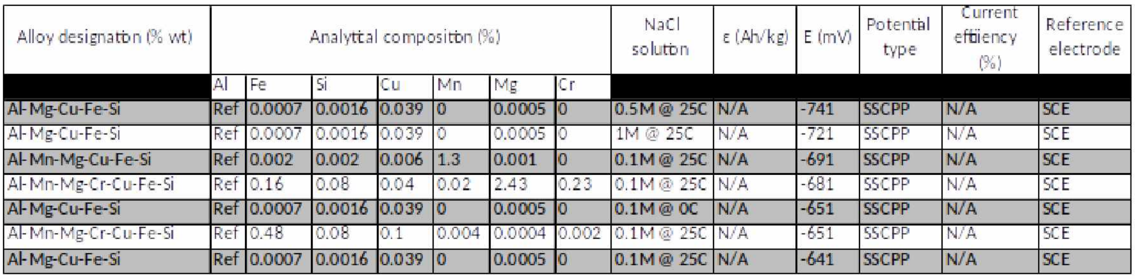

Alloy designation (% wt)	Analytical composition (%)							NaCl solution	ε (Ah/kg)	E (mV)	Potential type	Current efficiency (%)	Reference electrode
	Al	Fe	Si	Cu	Mn	Mg	Cr						
Al-Mg-Cu-Fe-Si	Ref	0.0007	0.0016	0.039	0	0.0005	0	0.5M @ 25C	N/A	-741	SSCPP	N/A	SCE
Al-Mg-Cu-Fe-Si	Ref	0.0007	0.0016	0.039	0	0.0005	0	1M @ 25C	N/A	-721	SSCPP	N/A	SCE
Al-Mn-Mg-Cu-Fe-Si	Ref	0.002	0.002	0.006	1.3	0.001	0	0.1M @ 25C	N/A	-691	SSCPP	N/A	SCE
Al-Mn-Mg-Cr-Cu-Fe-Si	Ref	0.16	0.08	0.04	0.02	2.43	0.23	0.1M @ 25C	N/A	-681	SSCPP	N/A	SCE
Al-Mg-Cu-Fe-Si	Ref	0.0007	0.0016	0.039	0	0.0005	0	0.1M @ 0C	N/A	-651	SSCPP	N/A	SCE
Al-Mn-Mg-Cr-Cu-Fe-Si	Ref	0.48	0.08	0.1	0.004	0.0004	0.002	0.1M @ 25C	N/A	-651	SSCPP	N/A	SCE
Al-Mg-Cu-Fe-Si	Ref	0.0007	0.0016	0.039	0	0.0005	0	0.1M @ 25C	N/A	-641	SSCPP	N/A	SCE

4.4 An overview of activation mechanisms

The focus of Researchers nowadays is on understanding the activation mechanisms, i.e. the ways that the various elements disrupt the formation of a stable oxide layer on the outer surface of the anode.

Table 4.37: Electrochemical performance of experimental compositions – Sharma et al ((Sharma, 2011)) / Table C.

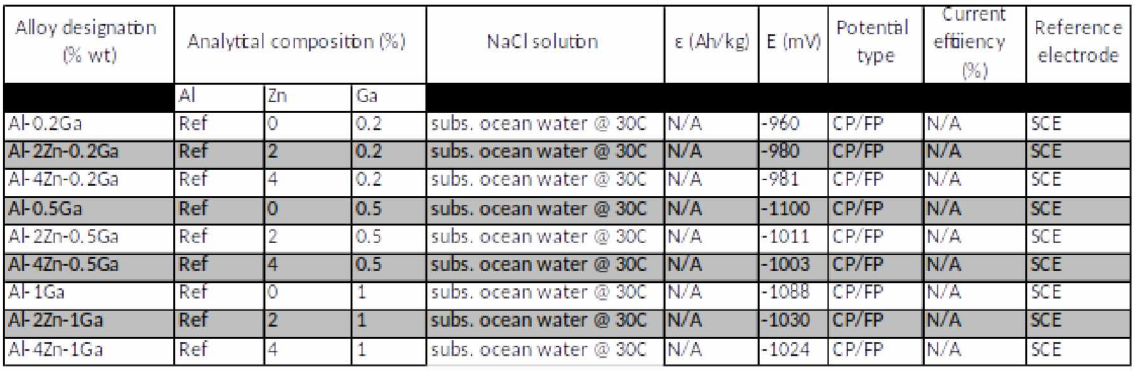

Alloy designation (% wt)	Analytical composition (%)			NaCl solution	ε (Ah/kg)	E (mV)	Potential type	Current efficiency (%)	Reference electrode
	Al	Zn	Ga						
Al-0.2Ga	Ref	0	0.2	subs. ocean water @ 30C	N/A	-960	CP/FP	N/A	SCE
Al-2Zn-0.2Ga	Ref	2	0.2	subs. ocean water @ 30C	N/A	-980	CP/FP	N/A	SCE
Al-4Zn-0.2Ga	Ref	4	0.2	subs. ocean water @ 30C	N/A	-981	CP/FP	N/A	SCE
Al-0.5Ga	Ref	0	0.5	subs. ocean water @ 30C	N/A	-1100	CP/FP	N/A	SCE
Al-2Zn-0.5Ga	Ref	2	0.5	subs. ocean water @ 30C	N/A	-1011	CP/FP	N/A	SCE
Al-4Zn-0.5Ga	Ref	4	0.5	subs. ocean water @ 30C	N/A	-1003	CP/FP	N/A	SCE
Al-1Ga	Ref	0	1	subs. ocean water @ 30C	N/A	-1088	CP/FP	N/A	SCE
Al-2Zn-1Ga	Ref	2	1	subs. ocean water @ 30C	N/A	-1030	CP/FP	N/A	SCE
Al-4Zn-1Ga	Ref	4	1	subs. ocean water @ 30C	N/A	-1024	CP/FP	N/A	SCE

Table 4.38: Electrochemical performance of experimental compositions – Sharma et al ((Sharma, 2011)) / Table D.

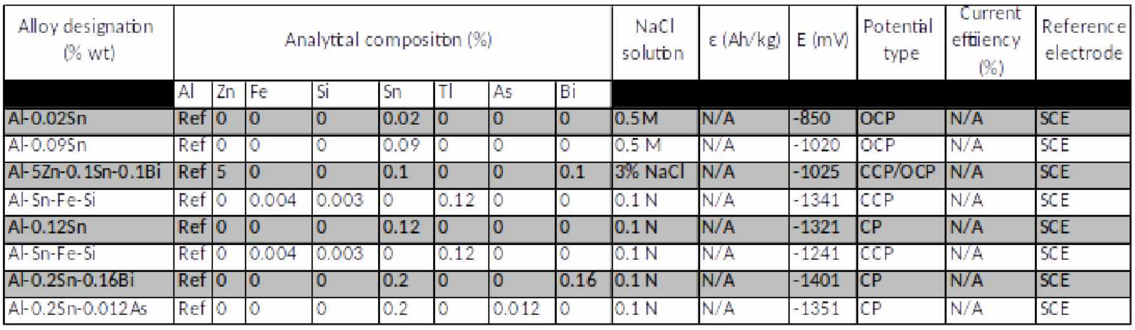

Alloy designation (% wt)	Analytical composition (%)								NaCl solution	ε (Ah/kg)	E (mV)	Potential type	Current efficiency (%)	Reference electrode
	Al	Zn	Fe	Si	Sn	Tl	As	Bi						
Al-0.02Sn	Ref	0	0	0	0.02	0	0	0	0.5M	N/A	-850	OCP	N/A	SCE
Al-0.09Sn	Ref	0	0	0	0.09	0	0	0	0.5 M	N/A	-1020	OCP	N/A	SCE
Al-5Zn-0.1Sn-0.1Bi	Ref	5	0	0	0.1	0	0	0.1	3% NaCl	N/A	-1025	CCP/OCP	N/A	SCE
Al-Sn-Fe-Si	Ref	0	0.004	0.003	0	0.12	0	0	0.1 N	N/A	-1341	CCP	N/A	SCE
Al-0.12Sn	Ref	0	0	0	0.12	0	0	0	0.1 N	N/A	-1321	CP	N/A	SCE
Al-Sn-Fe-Si	Ref	0	0.004	0.003	0	0.12	0	0	0.1 N	N/A	-1241	CCP	N/A	SCE
Al-0.2Sn-0.16Bi	Ref	0	0	0	0.2	0	0	0.16	0.1 N	N/A	-1401	CP	N/A	SCE
Al-0.2Sn-0.012As	Ref	0	0	0	0.2	0	0.012	0	0.1 N	N/A	-1351	CP	N/A	SCE

Table 4.39: Electrochemical performance of experimental compositions – Sharma et al ((Sharma, 2011)) / Table E.

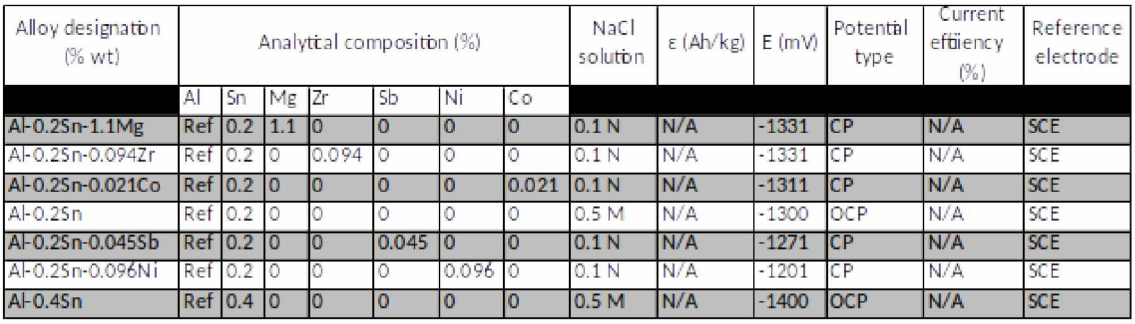

Alloy designation (% wt)	Analytical composition (%)							NaCl solution	ε (Ah/kg)	E (mV)	Potential type	Current efficiency (%)	Reference electrode
	Al	Sn	Mg	Zr	Sb	Ni	Co						
Al-0.2Sn-1.1Mg	Ref	0.2	1.1	0	0	0	0	0.1 N	N/A	-1331	CP	N/A	SCE
Al-0.2Sn-0.094Zr	Ref	0.2	0	0.094	0	0	0	0.1 N	N/A	-1331	CP	N/A	SCE
Al-0.2Sn-0.021Co	Ref	0.2	0	0	0	0	0.021	0.1 N	N/A	-1311	CP	N/A	SCE
Al-0.2Sn	Ref	0.2	0	0	0	0	0	0.5 M	N/A	-1300	OCP	N/A	SCE
Al-0.2Sn-0.045Sb	Ref	0.2	0	0	0.045	0	0	0.1 N	N/A	-1271	CP	N/A	SCE
Al-0.2Sn-0.096Ni	Ref	0.2	0	0	0	0.096	0	0.1 N	N/A	-1201	CP	N/A	SCE
Al-0.4Sn	Ref	0.4	0	0	0	0	0	0.5 M	N/A	-1400	OCP	N/A	SCE

The findings presented on different papers sometimes are inconclusive and different activation mechanisms have been assigned to the same element.

In other cases, the proposed mechanisms are not fully understood due to a lack of instrumentation or the difficulty of isolating and identifying the effect of a single element and as a result a vague estimation on the activation mechanism of an element is given.

An element that has been adequately researched and its activation mechanisms documented is Gallium. The prevailing activation mechanism theory for gallium is the discrete-particle mechanism and can be seen schematically on figure 4.4.

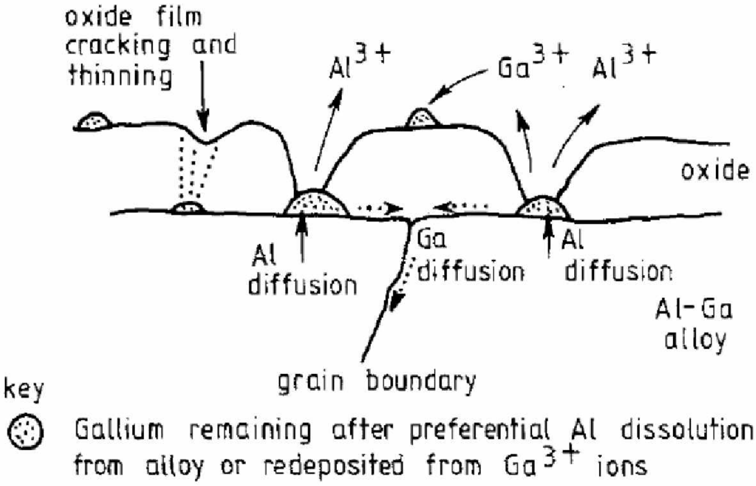

Figure 4.4: Gallium discete particle activation mechanism ((7$_b$, 2016))

Monzel et al ((Monzel and Druschitz, 2014)) recorder and presented the prevailing activation mechanism theories for various elements, as can be seen on figure 4.5.

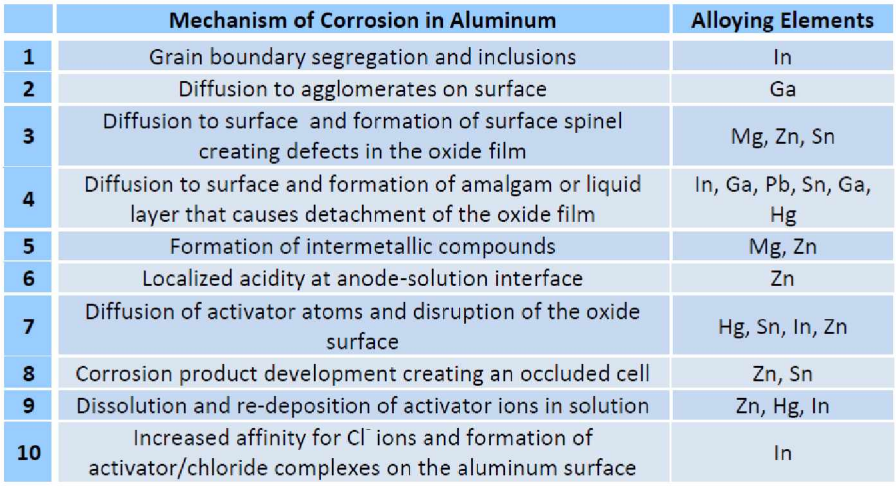

	Mechanism of Corrosion in Aluminum	Alloying Elements
1	Grain boundary segregation and inclusions	In
2	Diffusion to agglomerates on surface	Ga
3	Diffusion to surface and formation of surface spinel creating defects in the oxide film	Mg, Zn, Sn
4	Diffusion to surface and formation of amalgam or liquid layer that causes detachment of the oxide film	In, Ga, Pb, Sn, Ga, Hg
5	Formation of intermetallic compounds	Mg, Zn
6	Localized acidity at anode-solution interface	Zn
7	Diffusion of activator atoms and disruption of the oxide surface	Hg, Sn, In, Zn
8	Corrosion product development creating an occluded cell	Zn, Sn
9	Dissolution and re-deposition of activator ions in solution	Zn, Hg, In
10	Increased affinity for Cl^- ions and formation of activator/chloride complexes on the aluminum surface	In

Figure 4.5: Proposed activation mechanisms for various elements. ((Monzel and Druschitz, 2014))

Chapter 5

Future trends

Cathodic Protection with the use of sacrificial anodes has been utilized for decades and as a result all the processes and components involved are highly optimized, leaving only few areas where substantial improvements can be achieved.

55 years have passed since Reding and Newport's milestone study in the performance of aluminum based sacrificial anodes and the research is still ongoing. The trial-and-error approach of the past has yielded invaluable knowledge but is unlikely to be the research pattern of the future, since many elements have already been exhaustively researched, forcing researchers to experiment with unconventional materials, such as metal oxides (IRO_2, RuO_2, CeO_2) and rare earth elements (Lanthanum).

The goal of modern studies shifts away from the pursuit of absolute electrochemical performance and focuses on acquiring knowledge on the corrosion mechanisms that sacrificial anodes with different compositions exhibit in saline solutions and identify the effect of individual and multiple element additions in Aluminum sacrificial anodes. Another area of interest is the successful elimination of the adverse effects of Aluminum impurities, such as Iron and Copper, a prospect that could allow the use of lower purity aluminum without performance loss.

Extensive research on the metallurgical aspects of sacrificial anode manufacture, from casting and cooling parameters to the proper distribution of alloying elements, has yielded promising results and is an area where optimization could lead to better sacrificial anodes with a smaller energy and resource footprint.

Nowadays, Al-Zn-In sacrificial anodes are the prevalent option in commercial offshore applications, owing to their high electrochemical performance, uniform corrosion, ease of manufacture and non-toxicity, a status quo that is unlikely to change. Other promising compositions must surpass the established Al-Zn-In in every aspect and as a result the task to identify a replacement for Al-Zn-In sacrificial anodes is quite an undertake.

Bibliography

Understanding the Corrosion of Low-Voltage Al-Ga Anodes, volume All Days of *NACE CORROSION*, 03 2016.

G. .A. Performance of aluminium anode by addition of zinc in sea water-a review. 05 2018.

A. Barbucci, G. Cerisola, G. Bruzzone, and A. Saccone. Activation of aluminium anodes by the presence of intermetallic compounds. *Electrochimica Acta*, 42(15):2369–2380, 1997. ISSN 0013-4686. doi: https://doi.org/10.1016/S0013-4686(96)00420-3.

E. Bardal. Corrosion and protection. page 315, 2004.

P. Bonora, S. Rossi, L. Benedetti, and M. Draghetti. 11 - improved sacrificial anodes for the protection of offshore structures. In S. Campbell, N. Campbell, and F. Walsh, editors, *Developments in Marine Corrosion*, Woodhead Publishing Series in Metals and Surface Engineering, pages 155–162. Woodhead Publishing, 1998. ISBN 978-1-85573-825-6. doi: https://doi.org/10.1533/9781845698768.155.

C. B. Breslin and W. M. Carroll. The electrochemical behaviour of aluminium activated by gallium in aqueous electrolytes. *Corrosion Science*, 33(11):1735–1746, 1992. ISSN 0010-938X. doi: https://doi.org/10.1016/0010-938X(92)90005-N.

G. Bruzzone, A. Barbucci, and G. Cerisola. Effect of intermetallic compounds on the activation of aluminium anodes. *Journal of Alloys and Compounds*, 247(1):210–216, 1997. ISSN 0925-8388. doi: https://doi.org/10.1016/S0925-8388(96)02601-1.

V. Cicek. Cathodic protection: Industrial solutions for protecting against corrosion. 2013.

A. H. Committee. *Properties and Selection: Nonferrous Alloys and Special-Purpose Materials*. ASM International, 01 1990. ISBN 978-1-62708-162-7. doi: 10.31399/asm.hb.v02.9781627081627.

S. Cramer and B. Covino. *ASM Handbook, Volume 13A: Corrosion: Fundamentals, Testing, and Protection*. ASM Handbook Series. ASM International, 2003. ISBN 9780871707055.

R. Crundwell. 4.19 - sacrificial anodes. In B. Cottis, M. Graham, R. Lindsay, S. Lyon, T. Richardson, D. Scantlebury, and H. Stott, editors, *Shreir's Corrosion*, pages 2763–2780. Elsevier, Oxford, 2010. ISBN 978-0-444-52787-5. doi: https://doi.org/10.1016/B978-044452787-5.00153-0.

A. Farooq, M. Hamza, Q. Ahmed, and K. M. Deen. Evaluating the performance of zinc and aluminum sacrificial anodes in artificial seawater. *Electrochimica Acta*, 314:135–141, 2019. ISSN 0013-4686. doi: https://doi.org/10.1016/j.electacta.2019.05.067.

D. Flamini and S. Saidman. Electrochemical behaviour of al–zn–ga and al–in–ga alloys in chloride media. *Materials Chemistry and Physics*, 136(1):103–111, 2012. ISSN 0254-0584. doi: https://doi.org/10.1016/j.matchemphys.2012.06.036.

Gamry. Gamry White Papers-Guides to Electrochemistry Applications, 2021. URL `https://www.gamry.com/resources/white-papers/`.

J. guang HE, J. ba WEN, X. dong LI, G. wei WANG, and C. hua XU. Influence of ga and bi on electrochemical performance of al-zn-sn sacrificial anodes. *Transactions of Nonferrous Metals Society of China*, 21(7):1580–1586, 2011. ISSN 1003-6326. doi: https://doi.org/10.1016/S1003-6326(11)60900-X.

J. He, J. Wen, and X. Li. Effects of precipitates on the electrochemical performance of al sacrificial anode. *Corrosion Science*, 53(5):1948–1953, 2011. ISSN 0010-938X. doi: https://doi.org/10.1016/j.corsci.2011.02.016.

N. Idusuyi and L. Oluwole. Aluminium sacrificial anode activation – a review. *International Journal of Science and Technology*, 2:561–566, 01 2012.

A. Keyvani, M. Emamy, M. Saremi, H. Sina, and M. Mahta. Influence of casting temperature on electrochemical behavior of al-zn-in sacrificial anodes. *Iran. J. Chem. Chem. Eng.*, 24:1–8, 09 2005.

S. Lindsay. Very high purity aluminum: An historical perspective. *JOM*, 66, 02 2014. doi: 10.1007/s11837-013-0843-5.

J. Ma and J. Wen. The effects of lanthanum on microstructure and electrochemical properties of al–zn–in based sacrificial anode alloys. *Corrosion Science*, 51(9):2115–2119, 2009. ISSN 0010-938X. doi: https://doi.org/10.1016/j.corsci.2009.05.039.

J. Ma and J. Wen. Corrosion analysis of al–zn–in–mg–ti–mn sacrificial anode alloy. *Journal of Alloys and Compounds*, 496(1):110–115, 2010. ISSN 0925-8388. doi: https://doi.org/10.1016/j.jallcom.2010.02.174.

J. Ma, J. Wen, W. Zhai, and Q. Li. In situ corrosion analysis of al-zn-in-mg-ti-ce sacrificial anode alloy. *Materials Characterization*, 65:86–92, 2012. ISSN 1044-5803. doi: https://doi.org/10.1016/j.matchar.2012.01.003.

L. Ma, K. Li, Y. Yan, and B. Hou. Low driving voltage aluminum alloy anode for cathodic protection of high strength steel. *Advanced Materials Research*, 79-82:1047 – 1050, 2009.

C. D. Mance A. and M. A. The effect of small additions of indium and thallium on the corrosion behaviour of aluminium in sea water. pages 459–466, 1984. doi: https://doi.org/10.1007/BF00610810.

W. Monzel and A. Druschitz. Investigation of new, low-voltage, aluminum, sacrificial anode chemistries. 2014.

J. C. Norris, J. D. Scantlebury, M. R. Alexander, C. J. Blomfield, and R. F. Crundwell. Quantitative analysis of indium and iron at the surface of a commercial al–zn–in sacrificial anode. *Surface and Interface Analysis*, 30(1):170–175, 2000. doi: https://doi.org/10.1002/1096-9918(200008)30:1⟨170::AID-SIA733⟩3.0.CO;2-W.

D. Norske Veritas. RECOMMENDED PRACTICE CATHODIC PROTECTION DESIGN. 2010.

PalmSens. Knowledgebase - PalmSens, 2021. URL `https://www.palmsens.com/knowledgebase-article/`.

M. Pourgharibshahi and M. Meratian. Corrosion morphology of aluminium sacrificial anodes. *Materials and Corrosion*, 65(12):1188–1193, 2014. doi: https://doi.org/10.1002/maco.201307173.

M. R. Saeri and A. Keyvani. Optimization of manganese and magnesium contents in as-cast aluminum-zinc-indium alloy as sacrificial anode. *Journal of Materials Science & Technology*, 27(9):785–792, 2011. ISSN 1005-0302. doi: https://doi.org/10.1016/S1005-0302(11)60143-6.

M. Saremi, A. Keyvani, H. Sina, and M. Emamy. Improvement of the current capacity of al-zn-in anode by casting parameters and magnesium addition. 01 2004.

A. Sharma. Ab initio and thermodynamic modelling of alloying effects on activity of sacrificial aluminium anodes. *Corrosion Science*, 53(5):1724–1731, 2011. ISSN 0010-938X. doi: https://doi.org/10.1016/j.corsci.2011.01.046.

L. Sherwood. 10.2 – sacrificial anodes. 1994.

S. Shibli and V. Gireesh. Surface activation of aluminium alloy sacrificial anodes by iro2. *Applied Surface Science*, 219(3):203–210, 2003. ISSN 0169-4332. doi: https://doi.org/10.1016/S0169-4332(03)00675-5.

S. Shibli and V. Gireesh. Activation of aluminium alloy sacrificial anodes by selenium. *Corrosion Science*, 47(8):2091–2097, 2005. ISSN 0010-938X. doi: https://doi.org/10.1016/j.corsci.2004.09.010.

S. Shibli, V. Gireesh, and S. George. Surface catalysis based on ruthenium dioxide for effective activation of aluminium sacrificial anodes. *Corrosion Science*, 46(4):819–830, 2004. ISSN 0010-938X. doi: https://doi.org/10.1016/S0010-938X(03)00038-6.

S. Shibli, B. Jabeera, and R. Manu. Development of high performance aluminium alloy sacrificial anodes reinforced with metal oxides. *Materials Letters - MATER LETT*, 61: 3000–3004, 06 2007. doi: 10.1016/j.matlet.2006.10.062.

S. Shibli, S. Archana, and P. Muhamed Ashraf. Development of nano cerium oxide incorporated aluminium alloy sacrificial anode for marine applications. *Corrosion Science*, 50(8):2232–2238, 2008. ISSN 0010-938X. doi: https://doi.org/10.1016/j.corsci.2008.06.017.

Swain. Appendix: Cathodic Protection Design-1. 1996.

K. Toda, T. Murai, C. Miura, Y. Tamura, M. Kinzoku Kogyo Kabushiki Kaisha, and N. Boshoku Kogy Kabushiki Kaisha. Aluminum alloy for galvanic anode. 45(186): 521, 10 1971.

T.-M. Tsai. Protection of steel using aluminium sacrificial anodes in artificial seawater. pages 17–21, 1996.

J. Wen, J. He, and X. Lu. Influence of silicon on the corrosion behaviour of al–zn–in–mg–ti sacrificial anode. *Corrosion Science*, 53(11):3861–3865, 2011. ISSN 0010-938X. doi: https://doi.org/10.1016/j.corsci.2011.07.039.

Z. Xia, W. Zhang, X. Yang, T. Chen, Y. Zhu, H. Ma, and L. Li. Influence of sn, cd, and si addition on the electrochemical performance of al–zn–in sacrificial anodes. *Materials and Corrosion*, 71(4):585–592. doi: https://doi.org/10.1002/maco.201911336.

X. G. Zhang. *Galvanic Corrosion*, chapter 10, pages 123–143. John Wiley & Sons, Ltd, 2011. ISBN 9780470872864. doi: https://doi.org/10.1002/9780470872864.ch10.